沸騰の伝播現象を利用したマイクロポンプの実用化

（課題番号　１３５５５０５３）

平成１３年度～平成１４年度科学研究費補助金（基盤研究(B)(2)）

研究成果報告書

平成１５年３月

研究代表者　　飯田　嘉宏
（横浜国立大学大学院工学研究院教授）

はしがき

研究組織

研究代表者　：　飯田嘉宏（横浜国立大学大学院工学研究院教授）

研究分担者　：　奥山邦人（横浜国立大学大学院工学研究院助教授）

研究経費

平成１３年度　：　6,900　千円

平成１４年度　：　3,100　千円

計　　10,000　千円

研究発表

（１）学会誌等

K.Okuyama, R.Takehara, J.Kim and Y.Iida, Micropump Using Boiling Propagation Phenomena, *Thermal Science and Engineering*, Vol.10, No.4 (2002), pp.19-20.

その他投稿準備中

（２）口頭発表

１）奥山邦人・入倉篤史・竹原令雄・金　政君・飯田嘉宏、沸騰の伝播現象を利用したマイクロポンプに関する研究、日本機械学会2001年度年次大会講演論文集、Vol.5 (2001), pp.193-194.

２）奥山邦人・竹原令雄・金　政君・飯田　嘉宏、沸騰の伝播現象を利用したマイクロポンプの基礎研究、第39回日本伝熱シンポジウム講演論文集、Vol.1 (2002), pp.157-158.

３）金　政君・奥山邦人・飯田嘉宏、急速沸騰を用いたマイクロアクチュエータにおける繰返し加熱の許容周波数、第39回日本伝熱シンポジウム講演論文集 Vol.3 (2002), pp.761-762.

その他研究発表予定

（３）出版物

なし

研　究　成　果

本研究の成果は、前ページの研究発表に掲げたものに加え、今後発表予定のものである。そこで、すでに研究発表したものの論文の写しを掲載するとともに、今までに得られている結果で未発表のものの一部を加えて以下に示す。

1）学会誌等発表論文

K.Okuyama, R.Takehara, J.H.Kim and Y.Iida, Micropump Using Boiling Propagation Phenomena, *Thermal Science and Engineering*, Vol.10, No.4 (2002), pp.19-20.

2）口頭発表論文

奥山邦人・入倉篤史・竹原令雄・金　政君・飯田嘉宏、沸騰の伝播現象を利用したマイクロポンプに関する研究、日本機械学会2001年度年次大会講演論文集、Vol.5 (2001), pp.193-194.

3）口頭発表論文

奥山邦人・竹原令雄・金　政君・飯田　嘉宏、沸騰の伝播現象を利用したマイクロポンプの基礎研究、第39回日本伝熱シンポジウム講演論文集、Vol.1(2002), pp.157-158.

4）口頭発表論文

金　政君・奥山邦人・飯田嘉宏、急速沸騰を用いたマイクロアクチュエータにおける繰返し加熱の許容周波数、第39回日本伝熱シンポジウム講演論文集、Vol.3 (2002), pp.761-762.

5）研究成果で未発表のものの一部（その１）

K.Okuyama, R.Takehara, J.H.Kim and Y.Iida, Pump Action by Boiling Propagation Phenomena in a Microchannel.

6）研究成果で未発表のものの一部（その２）

K.Okuyama, J.H.Kim and Y.Iida, Allowable Repetition Frequency of Pulse Heating in Microactuators Using Rapid Boiling (Effects of heater size and substrate material).

Micropump Using Boiling Propagation Phenomena*

Kunito OKUYAMA†, Reo TAKEHARA†, Jeong-Hun KIM† and Yoshihiro IIDA†

Key Words: *Boiling Propagation Phenomena, Micropump*

1 Introduction

In micropumps which use liquid-vapor phase change, the nozzle and/or diffuser structure next to the heater or the plural heaters along the channel are usually used to obtain the unidirectional net flow[1-4]. A new concept is associated with a peculiar boiling initiation phenomena which occurs in highly wetting liquids[5]. Figure 1 shows photographs just subsequent to boiling incipience of ethyl alcohol on a platinum film heater having a width of 1 mm heated stepwise. Successive activation of bubble nuclei occurs in the region adjacent to the preceding nucleated bubbles. The authors confirmed the pumping action produced by this phenomena in a microchannel, referred to as boiling propagation, by realizing a unidirectional propagation[6]. Continuous liquid transport may be feasible for a single heater in the channel having no uneven structure by the repetition of boiling propagation.

In the present study, the basic characteristics of the boiling propagation were investigated using a heater smaller than that in Fig.1. Pulse heating was repeated at a prescribed frequency under the condition with triggering for the propagation in a microchannel and the resultant pumping action was evaluated.

2 Experimental apparatus and procedure

Figures 2 and 3 show schematic diagrams of the test section and the experimental apparatus, respectively. The heater is a platinum film evaporated on a quartz glass substrate having a 0.2 mm × 2 mm heating area. A microchannel of which both the height and width are 0.25 mm is composed on the heater using a rubber sheet having a slit, a perforated acrylic resin plate, and glass tubes. Thermal ink jet printer ink (without dye) at room temperature is poured into the U-shaped channel. A constant pulse current is supplied to the heater at a prescribed frequency, and the boiling propagation is triggered by the bubble generated at one tip of the

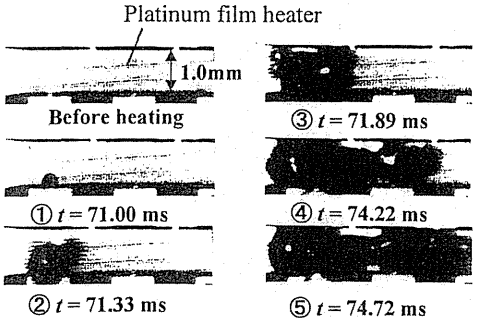

Fig.1 Boiling inception and propagation on the film heater

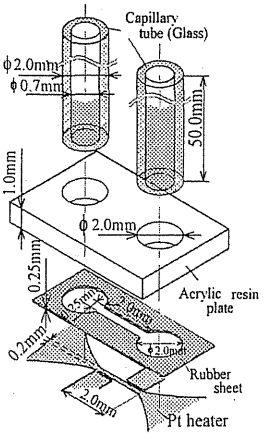

Fig.2 Schematic diagram of the test section

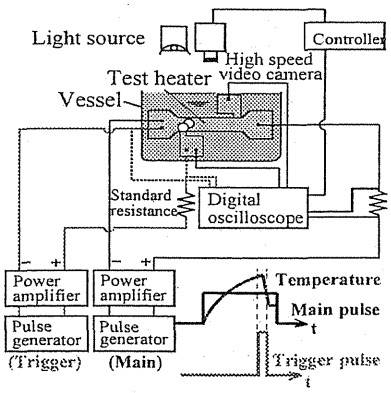

Fig.3 Schematic diagram of the experimental apparatus

* Received : June 11, 2002, Editor : Hiroshi KAWAMURA

† Department of Chemical Engineering Science, Yokohama National University (79-5 Tokiwadai, Hodogaya-ku, Yokohama 240-8501, JAPAN)

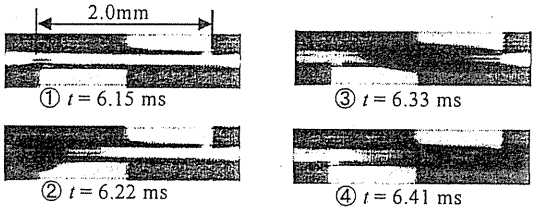

$\Delta T_{sat,trig} = 98.2$K, $Q = 3.91$ MW/m^2

Fig.4 Configuration of boiling caused by triggering

voltage taps via an additional short pulse when the heater reaches a prescribed superheat. The pumping action was evaluated based on the head difference generated between the liquid columns. The pulse power was obtained from the heating current and the resistance, and the heater temperature was obtained from the resistance variation. A high-speed video camera was used for the observation.

3 Experimental results

Boiling occurred at a pulse power Q higher than 1.3 MW/m^2 and at a wall superheat higher than 50 K without the triggering bubble. As seen in Fig.4, as soon as the triggering bubble is generated on the left tap, boiling is induced at the heater and propagates rapidly to the other end of the test section (in an open pool). The bubble was approximately 0.4 mm in height. Figure 5 shows the average propagation velocity $V_{p,av}$ plotted with respect to the wall superheat at the propagation $\Delta T_{sat,p}$ obtained by changing the wall superheat at the triggering $\Delta T_{sat,trig}$. $V_{p,av}$ increases significantly with $\Delta T_{sat,p}$. Figure 6 shows the time variation of the head difference ΔH during boiling propagation repeated at f=13 Hz. ΔH increases with time to reach the maximum value ΔH_{max} at approximately 30 s. After the termination of heating, the head difference recovers to the initial state. Figure 7 shows the head difference ΔH_{max} plotted with respect to the frequency f. ΔH_{max} increases with f and $\Delta T_{sat,trig}$ up to approximately 8.7 mm at f=20 Hz. However, as the frequency increases further, the pumping action was lost due to the significant increase in the substrate temperature around the heater, resulting in bubble generation at a random location prior to triggering.

4 Conclusions

A unidirectional boiling propagation has been realized by triggering during each heating pulse, based on the propagation characteristics. Continuous pumping action at a frequency up to 20 Hz has been demonstrated based on the head difference generated between liquid columns in the channel.

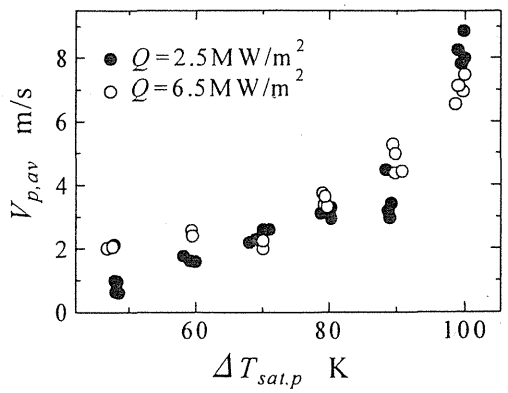

Fig.5 Relationship between average boiling propagation velocity and wall superheat

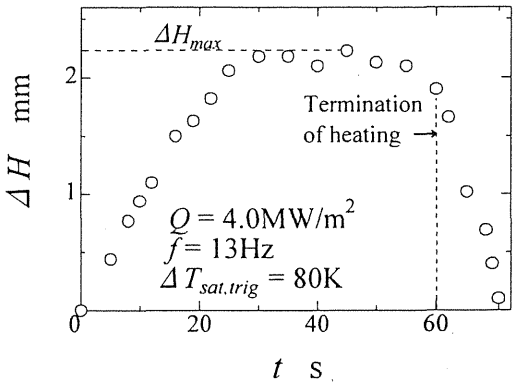

Fig.6 Time variation of head difference between liquid columns

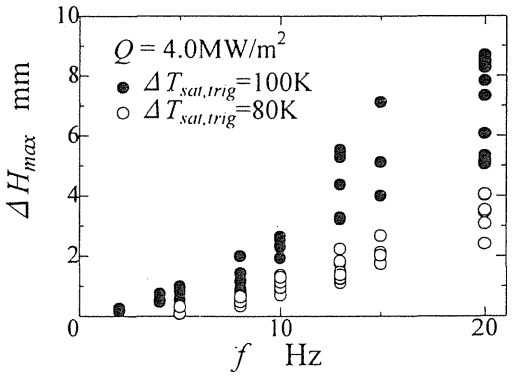

Fig.7 Relationship between maximum head difference between liquid columns and pulse heating repetition frequency

References

[1] Yang, W.J., Thermal Sci. & Engng., 9-4(2001), 3-8.
[2] Ozaki,K., Proc.IEEE MEMS, (1995), 31-36.
[3] Jun, T.K. and Kim, C.J., J. Appl. Phys., 83(1998), 5658-5664.
[4] Yuan, H. and Prosperetti, A., J. Micromech. Microengng., 9(1999), 402-413.
[5] Okuyama, K., Iida, Y. and Kato, T., Heat Transf. Jap. Res., 25(1996),51-63.
[6] Okuyama, K., Irikura, A., Takehara, R., Kim, J.H. and Iida Y., Proc. JSME, No.01-1, V(2001), 193-194.

K-1510 沸騰の伝播現象を利用したマイクロポンプに関する研究

Micropump using boiling propagation phenomena

正　奥山 邦人（横国大）　　○入倉 篤史（横国大院）
竹原 令雄（横国大院）　　金　政君（横国大院）
正　飯田 嘉宏（横国大）

Kunito OKUYAMA, Atushi IRIKURA, Reo TAKEHARA, Jeong Hun KIM and Yoshihiro IIDA
Dept. of Chemical Engineering Science, Yokohama National Univ., Hodogaya-ku, Yokohama

A prototype of new micropump which uses boiling propagation phenomenon is developed. Boiling is triggered on a film heater surface subjected to high pulse heating by generating a vapor bubble on an extremely high heat flux section, and the one-dimentional boiling propagation is realized along the entire length of the heater. Boiling configuration, propagation velocity and bubble height as well as the heating conditions on which the boiling propagation occurs are examined. Boiling propagated at the bottom in a U-shaped microchannel is demonstrated to produce a significant head difference between liquid columns in the vertical sections.

Key Words： Micropump, Boiling propagation, Film heater, Pulse heating

1. 緒　言

液－気相変化を利用したマイクロポンプは、(1)機械的駆動部をもたない、(2)発生圧力や体積膨張が大きい、(3)高い応答性をもつ、などの特徴があり、多くの研究が行われている。バブルは加熱毎に発生と消滅を繰り返すだけなので、マイクロ流路内で一方向に液を輸送するには、(1)バブル左右の流路に流れの非対称構造を設ける[1),2)]、(2)流路に沿って設けた複数のヒータを時系列加熱する[3),4),5)]、などの方法が提案されている。しかしこれらの方法は流路の構成やヒータの加熱方法が複雑になる。

一方、著者らは加熱面と高い濡れ性を有する液体において、沸騰開始時に加熱面に沿って沸騰領域が急速に広がる特異な「沸騰の伝播現象」が生じることとその特性を明らかにしてきた[6)]。この沸騰伝播現象を、Fig.1に示すように流路に沿った細長いヒータをパルス加熱し、その一端から発生させることができれば、(a)→(b)→(c)→(d)の順に発泡領域が推移することにより直管のマイクロ流路内での一方向への液体輸送が可能となると考えられる。

本報では、1mm×10mmの微小白金薄膜ヒータを急速加熱した際の伝播の発生条件、伝播形態、伝播速度、伝播気泡層高さ等を調べるとともに、ヒータの一端に設けた高熱流束部に発生させた気泡をトリガーとして一方向への沸騰の伝播現象の実現を計った。次にU字型マイクロ流路内で一方向への沸騰の伝播現象を発生させ、生じた左右液柱高さの差から本沸騰現象に基づくポンプ作用を明らかにした。

2. 実験装置及び方法

Fig.2に試験部、Fig.3に実験装置概略図をそれぞれ示す。主ヒータはガラス基板上に蒸着された厚さ0.2μmの白金薄膜で、1mm x10mmの発熱区間の両端に設けた２本の電圧タップのうち１本の先端縮小部を主ヒータ上の沸騰開始のためのバブル発生用トリガーヒータとしても用いる。白金薄膜ヒータ上にシリコンゴムシート、ガラス板を積層することにより、ヒータが流路の水平部分全長の側壁に位置する隙間1mm、幅1mmのU字型マイクロチャネルを形成して試料液(エタノール)を約7mmの高さまで満たす。単一矩形パルス信号を電力増幅して主ヒータを通電加熱し、ある過熱度まで上昇したときトリガーヒータを短時間加熱してバブルを発生させた。主ヒータの発熱量はタップ間電位差と加

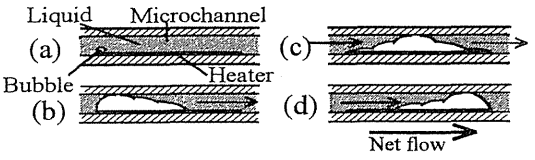

Fig.1　Principle of pumping mechanism by boiling propagation in microchannel

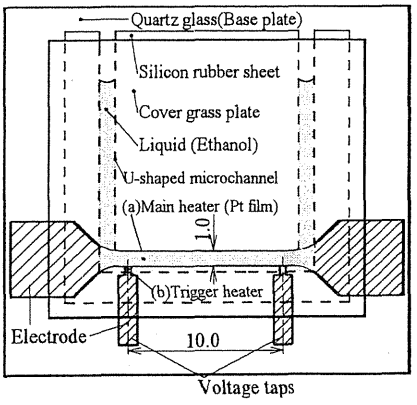

Fig.2　Test section

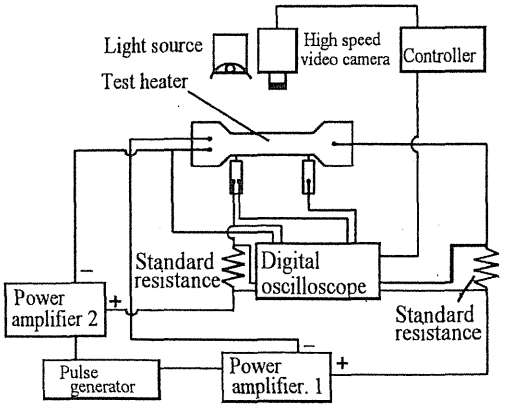

Fig.3　Schema of experimental apparatus

熱電流より、過熱度は電気抵抗変化より求めた。現象の観察にはハイスピードビデオカメラ(18000f/s)を用いた。なお、実験は室温、大気圧下で行った。

3. 実験結果

Fig.4は、流路を取り払ったバルク液中におけるパルス加熱時の主ヒータ上の沸騰様相の例を示す。Fig.4(a)はトリガ気泡なしの場合、Fig.4(b)はトリガ気泡を発生させた場合で、トリガ気泡なしでは極めて高過熱度で任意の場所から沸騰が開始し、ヒータ面に沿って伝播が生じて全面を気泡が覆うが、主ヒータ上で自発的な沸騰が始まる前にトリガ気泡を発生させるとそこから沸騰がヒータ面上を伝播して他端に達することがわかる。こうしてトリガ気泡により一方向への速やかな沸騰の伝播現象を実現できた。なお、トリガ気泡なしの条件では、0.5(MW/m^2)以上の発熱量(Q)で沸騰が生じ、沸騰開始時の伝熱面過熱度は約90K以上と極めて高い。Qが比較的小さい場合には1個の発生気泡から伝播現象が生じるが、2.0(MW/m^2)以上では複数の気泡が発生し、各気泡から伝播が開始した。また、側方からの観察により伝播気泡の平均高さhはQ = 0.5~2.0(MW/m^2)の間でh = 0.75~1.8mmであった。

Fig.5は、主ヒータ加熱中のトリガ気泡発生のタイミング(トリガー時主ヒータ過熱度$\Delta T_{sat,trig.}$)を様々に変化させた際の沸騰伝播開始時の伝熱面過熱度$\Delta T_{sat,p.}$と平均伝播速度$V_{p,avg.}$の関係を示す。$V_{p,avg.}$は$\Delta T_{sat,p.}$の増加に伴いほぼ直線的に増加する。なお、$\Delta T_{sat,trig.}$>90Kでは、トリガ気泡による沸騰が主ヒータ全面に伝播する途中で任意の場所から複数の気泡が発生した。

Fig.6は、ヒータ上に構成したマイクロチャネル内でトリガ気泡による沸騰伝播を発生させた際の様相を示す。t'は沸騰伝播開始時からの経過時間を示す。トリガ気泡発生①後、伝播気泡は主にヒータに沿った(水平)方向に成長し(②,③)、ヒータの他端に達している。この沸騰により左右両液柱は急激に押し上げられ、一時は内部が二相流状態となる。その後両液面は低下し、⑤の時刻では最大約9.7mmの液柱差が生じており、U字管の左から右へのポンプ作用が生じたことがわかる。⑥でほぼ初期の状態に戻っている。

Fig.7は、伝播速度$V_{p,avg.}$が大きく異なる$\Delta T_{sat,p.}$の二つの条件の場合について、伝播開始からの液柱高さの差ΔH_mの経時変化を示す。$\Delta T_{sat,p.}$=79.7Kの場合はFig.6の写真と対応している。伝播中は液柱差の増加速度が大きく、伝播が完了した後も緩やかに増加し続けること、伝播速度が大きいほど大きな液柱差が生じることがわかる。

4. 結　言

微小な白金薄膜ヒータを急速加熱した際の沸騰伝播現象の発生条件、伝播形態、伝播速度、伝播気泡層高さなどを調べるとともに、ヒータの一端に設けた高熱流束部に発生させた気泡をトリガーとする能動的な一方向への伝播現象を実現した。またU字型マイクロ流路内で一方向への沸騰の伝播現象を起こさせ、左右液柱高さの差から本現象が液体輸送機構として利用可能であることを示した。

【参考文献】

1) P. Gravesen et. al., J. Micromech. Microeng., 3(1993), 168.
2) A. Asai., Trans. ASME, 114(1992), 638.
3) K. Ozaki., Proc. MEMS'95, (1995), 31.
4) T.K. Jun and C.J. Kim., J.Appl. Phys., 83-11(1998), 5658.
5) H. Yuan and A. Prosperetti., J. Micromech. Microeng., 9(1999), 402.
6)奥山・飯田，機論(B)，62-595(1996)，1084.

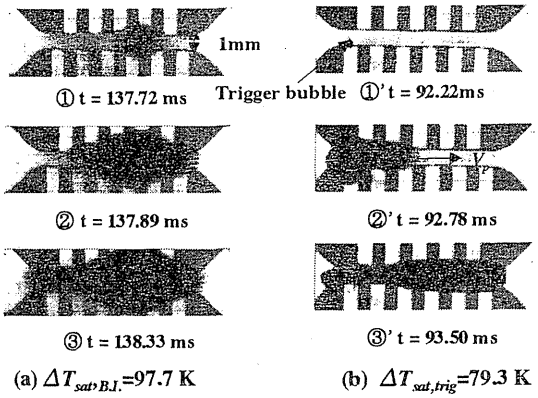

Fig.4 (a) Spontaneous and (b) triggered boiling inception and propagation

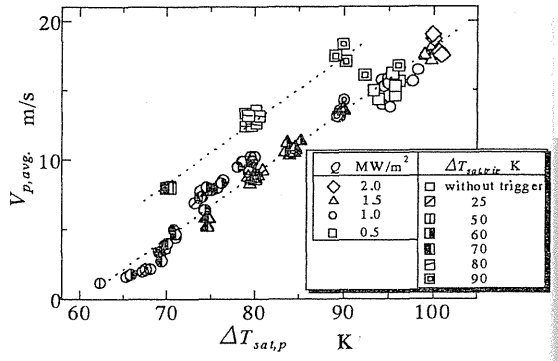

Fig.5 Relationship between average velocity of boiling propagation and wall superheat at boiling incipience

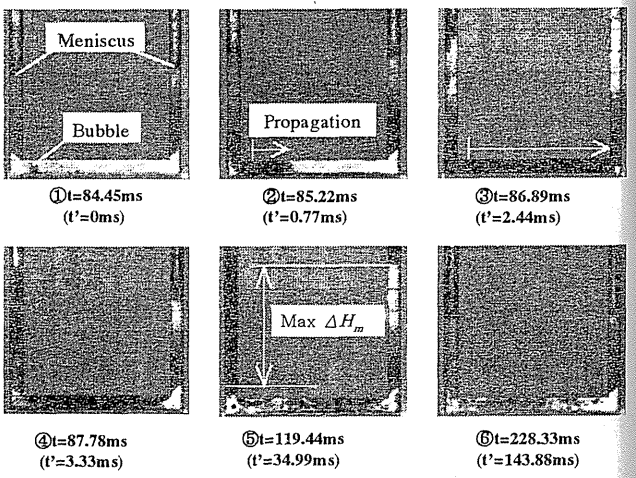

Fig.6 Boiling propagation in microchannel and movement of menisci (Q = 1.0MW/m^2, $\Delta T_{sat,p}$ = 79.7K)

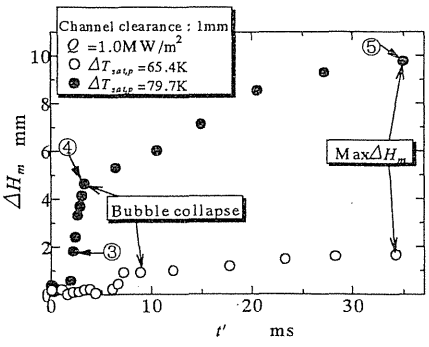

Fig.7 Time variation of difference between liquid column heights

E113

沸騰の伝播現象を利用したマイクロポンプの基礎研究

Micropump Using Boiling Propagation Phenomena

伝正　奥山 邦人（横国大・工）　　＊竹原 令雄（横国大院学）
金　政煮（横国大院学）　　伝正　飯田 嘉宏（横国大・工）

Kunito OKUYAMA, Reo TAKEHARA, Jeong-Hun KIM and Yoshihiro IIDA
Dept. of Chemical Engineering Science, Yokohama National Univ., Hodogaya-ku, Yokohama 240-8501

A prototype of new micropump which uses boiling propagation phenomena is developed. Boiling is triggered on a film heater surface subjected to high pulse heating by generating a vapor bubble on an extremely high heat flux section, and the one-directional boiling propagation is realized along the entire length of the heater. Boiling configuration, propagation velocity as well as the heating conditions on which the boiling propagation occurs are investigated. Continuous liquid transport is demonstrated in a microchannel by repeating the one-directional boiling propagation. Maximum head difference measured between liquid columns is 8.7mm for pulse heating repetition frequency 20Hz.

Key Words： Nucleate Boiling Propagation Phenomena, Micropump

1. はじめに

液気相変化を利用したマイクロポンプは、(1)機械的駆動部をもたない、(2)発生圧力や体積膨張が大きい、(3)高い応答性をもつ、などの特徴があり、多くの関心がもたれている。沸騰気泡は加熱毎に発生と消滅を繰り返すだけなので、流路内での一方向への液体輸送を可能にするため、(1)加熱部左右の流路形状の非対称化[1]、(2)流路に沿う複数のヒータの時系列加熱[2)-4)]などの方法が提案されているが、これらの場合、流路の形状やヒータの加熱方法が複雑になる。

一方、著者らは加熱面との高い濡れ性を有する液体において、沸騰開始時に加熱面に沿って沸騰領域が急速に広がる特異な「沸騰の伝播現象」が発生することを明らかにしている[5)]。Fig.1 に、ガラス基板上に蒸着した幅 1.0mm、長さ 11mm の白金薄膜ヒータをエタノールプール液中に浸漬し、パルス状に通電加熱した際の様相を示す。このときヒータの一端に設けた高熱流束部に短時間電流を流すことにより、伝熱面過熱度が 60K まで上昇したときに強制的に気泡を発生させ、その気泡をトリガとしてヒータ面上に沸騰を生起させた。発生した気泡が隣接箇所の気泡核を次々と活性化させる様に発泡が起こり、ヒータ面に沿って沸騰域が広がる様子がわかる。著者らはこのような現象を沸騰の伝播現象と呼んでおり、側壁に Fig.1 のヒータを持つ U 字型マイクロ流路内で一方向への沸騰伝播現象を発生させ、生じた左右液柱高さの差から本沸騰現象にポンプ作用があることを示した[6)]。このような現象を繰り返し発生させることができれば、凹凸形状を持たない直管のマイクロ流路内での単一のヒータ加熱による一方向へ液体の連続輸送ができる可能性があると考えられる。

本報では、ヒータからの放熱性を考慮し、Fig.1に示したものの幅、長さともに1/5の微小な白金薄膜ヒータを急速加熱し、その際の伝播の発生条件、伝播形態、伝播速度を調べるとともに、ヒータの一端に設けた高熱流束部に発生させた気泡をトリガとして一方向への沸騰の伝播現象の実現を計った。次にマイクロ流路内でヒータを一定の周波数で繰り返しパルス加熱し、この時生じた流路両端の液柱間ヘッド差からポンプ作用の大きさを調べた。

2. 実験装置及び方法

Fig.2に試験部、Fig.3に実験装置概略図をそれぞれ示す。ヒータはガラス基板上の厚さ0.2μmの白金蒸着薄膜で、0.2mmx2mmの発熱区間の端部に設けた２本の電圧タップのうち１本の先端縮小部をヒータ上の沸騰を誘発するための気泡発生用トリガ部としても用いる。白金薄膜ヒータ上にゴムシート、アクリル板、ガラス細管を積層することにより、マイクロチャネルを形成して試料液(プリンタ用インク(染料抜き))を満たす。矩形パルス信号を一定周波数で発生

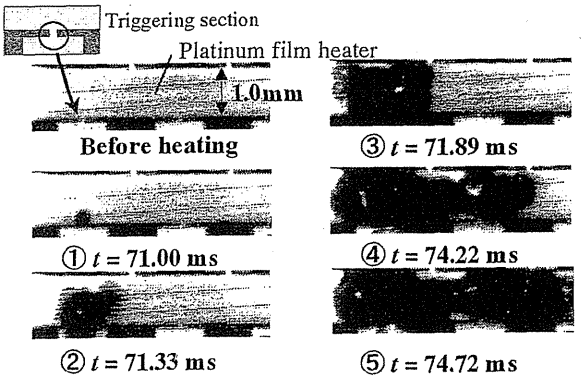

Ethyl alcohol, P= 0.1MPa, T_L=25℃, $\Delta T_{sat,B.I.}$= 61K

Fig.1　Boiling inception and propagation

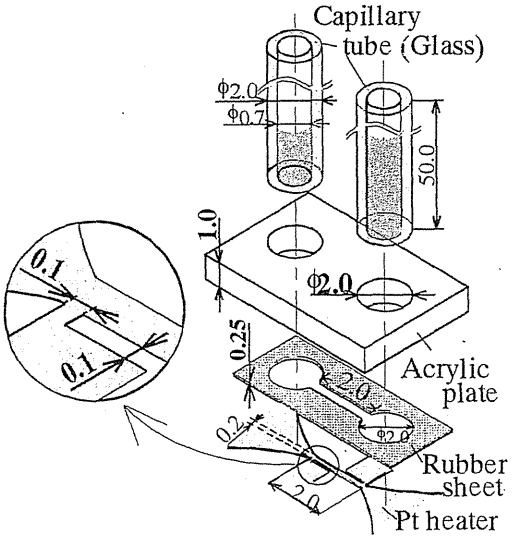

Fig.2　Schema of test section

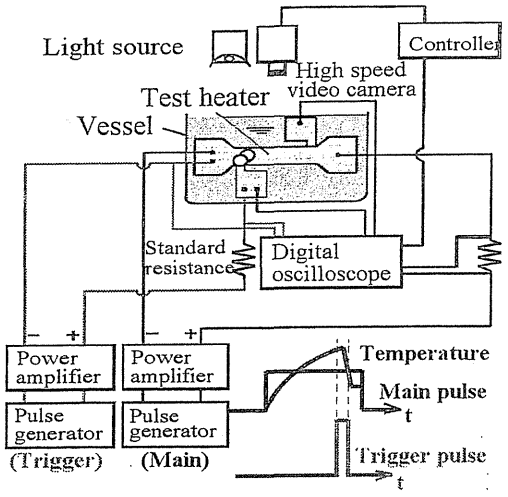

Fig.3 Schema of experimental apparatus

させ、これを電力増幅してヒータを通電加熱し、各パルス毎にヒータがある過熱度まで上昇したときトリガ部を短時間加熱して気泡を発生させた。ヒータの発熱量はタップ間電位差と加熱電流より、伝熱面温度は電気抵抗の温度変化より求めた。沸騰現象の観察にはハイスピードビデオカメラ(27000f/s)を用いた。実験は室温、大気圧下で行った。

3. 実験結果及び考察

ヒータの発熱量(熱流束換算値)Q=1.3(MW/m^2)以上のパルス加熱で沸騰が生じ始め、その際の伝熱面過熱度は約50K以上であった。Fig.4は、流路を取り払ったプール液中におけるパルス加熱時の様相の例を示す。伝熱面過熱度ΔT_{sat}が98.2Kの時トリガ気泡を発生させると、そこから速やかに沸騰が開始してヒータ面上を伝播し、他端に達することがわかる。このときの平均伝播速度は$V_{p,av}$=8.9m/sであった。こうしてトリガ気泡により一方向への速やかな沸騰の伝播現象を実現できた。

Fig.5はトリガ気泡発生時の伝熱面過熱度$\Delta T_{sat,trig}$を変化させた際の伝播開始時の伝熱面過熱度$\Delta T_{sat,p}$と$V_{p,av}$の関係を示す。$V_{p,av}$は$\Delta T_{sat,p}$の増加に伴い顕著な増加傾向を示す。

Fig.6は、ヒータ上に構成したマイクロチャネル内で、トリガ気泡による一方向への沸騰伝播現象を繰り返し加熱周波数f=13Hzにおいて発生させた際のガラス管内液柱間ヘッド差Hの時間変化を示す。繰り返し加熱開始後約30秒後にほぼ最大ヘッド差(H_{max})となる。加熱終了直前まで最大値を維持し、加熱終了後には速やかに初期の状態に戻った。

Fig.7は、繰り返し加熱周波数fに対するガラス管内液柱間の最大ヘッド差H_{max}を示す。fの増加とともにH_{max}は増加している。また、$\Delta T_{sat,trig}$が大きいほど大きなヘッド差が得られた。f=20Hzで最大約8.7mmの液柱ヘッド差が得られたが、さらにfを増加させると、連続する二つの加熱パルス間におけるヒータの温度が顕著に上昇し、後続するパルス加熱においてヒータ上の任意の場所から発泡し、ポンプ作用が急速に失われた。

4. 結　言

微小な白金薄膜ヒータを急速加熱した際の沸騰伝播現象の発生条件、伝播速度などを調べるとともに、ヒータの一端に設けた高熱流束部に発生させた気泡をトリガとする能動的な一方向への伝播現象を実現した。またマイクロチャネル内で一方向への沸騰の伝播現象を繰り返し発生させ、得られたヘッド差から本現象が液体輸送方法として応用可能であることを示した。

【参考文献】

1) Yang, W.J., Thermal Sci. & Engng., 9-4 (2001), 3.

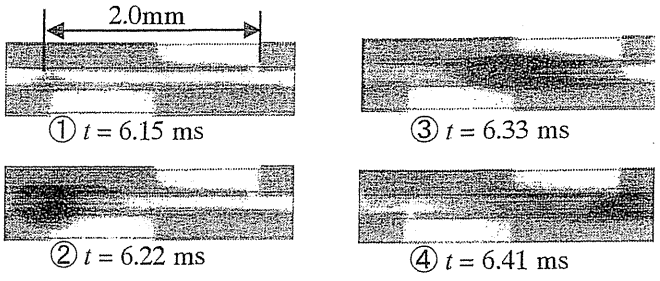

$\Delta T_{sat,trig}$ = 98.2K, Q = 3.91 MW/m^2

Fig.4 Configuration of boiling caused by triggering

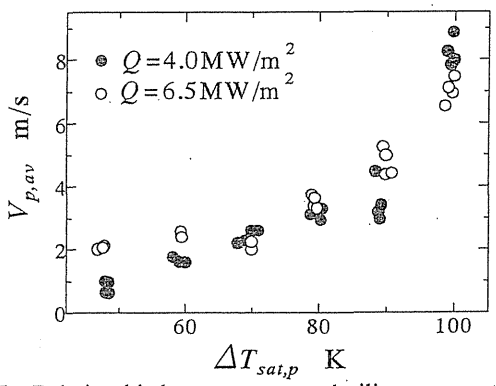

Fig.5 Relationship between average boiling propagation velocity and wall superheat

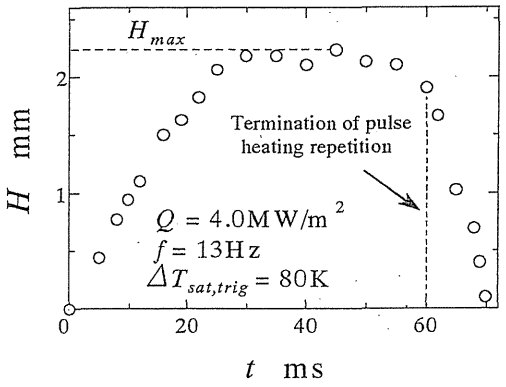

Fig.6 Time variation of head difference between liquid columns

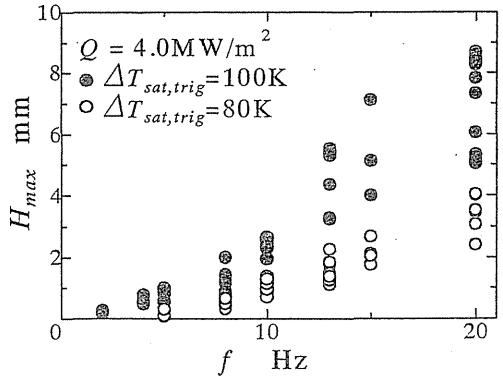

Fig.7 Relationship between maximum head difference between liquid columns and pulse heating repetition frequency

2) Ozaki, K., Proc. MEMS'95(1995), 31.
3) Jun, T.K. and Kim, C.J., J. Appl. Phys., 83-11(1998), 5658.
4) Yuan, H. and Prosperetti, A., J. Micromech. Microengng 9(1999), 402.
5) 奥山他，機論(B)，62-595(1996), 1084.
6) 奥山他，機講論，01-1, V (2001), 193.

G321

急速沸騰を用いたマイクロアクチュエータにおける繰返し加熱の許容周波数

Allowable Repetition Frequency of Pulse Heating in Microactuators using Rapid Boiling

＊金　政焄（横国大院学）　　正　奥山　邦人（横国大・工）
正　飯田　嘉宏（横国大・工）

Jeong-Hun KIM, Kunito OKUYAMA and Yoshihiro IIDA
Dept. of Chemical Engineering Science, Yokohama National Univ., Hodogaya-ku, Yokohama 240-8501

Maximum repetition frequency of pulse heating, at which the temperature increase on and around a film heater in microactuators using rapid boiling can be maintained within the allowable range during the succession of pulse heating, is estimated by the numerical simulation of the unsteady state thermal conduction of an axially symmetrical system. The size of the heater and the thermophysical properties of the surrounding media significantly affect the allowable frequency. The non-dimensionalized allowable frequency is approximated theoretically as a function of Fourier number. The prediction is well compared with the measured results.

Key Words : Microactuator, Rapid Boiling, Pulse Heating, Allowable Repetition Frequency, Numerical Simulation

1. 緒　言

急速沸騰を用いたマイクロアクチュエータは、サーマルインクジェット(TIJ)プリンタに実用化され、最近ではマイクロスラスタにもその適用が検討されている。しかし、短い周期でパルス加熱を繰り返すと、ヒータ及びその周囲の温度が徐々に上昇し、沸騰現象の再現性が失われたり、ヒータが劣化する恐れがある。このため、TIJプリンタでは、ヒータ付近の温度がある値まで上昇すると加熱を一時休止するなどしている[1]。ヒータの温度上昇を許容値以下に保ちながらパルス加熱毎の沸騰を再現性よく繰り返すことのできる最大周波数は、加熱パルスの高さや時間幅に加え、微小なヒータから周囲への放熱のし易さによると考えられる。スケーリング則[2]並びに著者らのこれまでの研究[3]-[5]によれば、マイクロサイズでは、熱伝達より熱伝導の効果が大きくなり、放熱は主として基板や気泡発生前及び消滅後の液体への熱伝導のみによると見なしても大きな問題は生じないものと考えられる。

そこで本研究では、液体に接する基板表面の微小薄膜ヒータの温度上昇(時間平均値)をある値以下に保つことのできる繰返し加熱周波数f_aを、3次元放熱効果が考慮できる円柱座標系2次元非定常熱伝導モデルによる数値計算で求め、無次元数による整理を試みた。また、近似予測式を導出し、これらの予測値を繰返しパルス加熱実験の結果と比較した。

2. 解析モデルおよび計算方法

Fig.1に示すように、十分大きな基板の表面に直径D_h(=2R_h)の薄い微小な円板状のヒータがあり、基板表面は十分な量の液体に接している系を考える。微小ヒータを一様かつパルス状に繰返し発熱させた際のヒータ及びその周囲の温度変化は、熱物性値一定の仮定の下で、以下の円柱座標系2次元非定常熱伝導基礎式を解くことにより求めることができる。

i) ヒータ：
$$\rho c_p \frac{\partial T}{\partial t} = \frac{k}{r}\frac{\partial}{\partial r}\left(r\frac{\partial T}{\partial r}\right) + Q''' \qquad (1.a)$$

ii) 基板及び液体：
$$(\rho c_p)_i \frac{\partial T_i}{\partial t} = \frac{k_i}{r}\frac{\partial}{\partial r}\left(r\frac{\partial T_i}{\partial r}\right) + k_i \frac{\partial}{\partial z}\left(\frac{\partial T_i}{\partial z}\right) \qquad (1.b)$$

ここで、i=1:working liquid, i=2:solid 1, i=3:solid 2である。式(1.a)、(1.b)を有限差分法で離散化し、初期温度一様、またr=0で$\partial T/\partial r = 0$及び$r=R_h+L_{re}$、$z=L_a$、$z=L_b$で温度一定の境界条件の下で完全陰解法により数値解を求めた。L_{re}, L_a, L_bは各加熱条件でのヒータの温度上昇に影響を与えないよう十分大きく取った。繰返し加熱の全過程について計算する代わりに、時間幅τの1回のパルス加熱で作動流体の自発核生成温度までの昇温(ΔT_τ)に要するパルス発熱量Q_p''と、繰り返しパルス加熱時のヒータの時間平均温度が予め設定した値まで上昇(ΔT_a)して定常状態になる時間平均発熱量Q_s''をそれぞれ繰返し計算により求め、結果をエネルギーバランス式、

$$Q_p'' f_a = Q_s'' \qquad (2)$$

に代入することによりf_aを求めた。なお、基板は二層から構成されるものとし、表1に示すように、Solid1,2について、ともにSiO_2の場合(Case I)、Siの場合(Case II)、それぞれSiO_2及びSiの場合(Case III)について、D_h、τ及びΔT_a、ΔT_τの値を種々変化させて計算を行った。Case IIIにおけるSiO_2層は、MEMSの加工技術によりマイクロヒータを形成する際のSi基板とヒータとの間の電気絶縁層に対応している。

3. 計算結果及び考察

まず、計算結果に対する諸因子の影響を明らかにするため、現象を支配する無次元量の推定を行った。同一ヒータでの異なるτにおける単一パルス加熱終了時(ΔT_τ=265K)のヒータ周りの等温線分布の例をFig.2に示す。これよりヒータ周囲への熱伝導は、ヒータ表面垂直方向1次元と仮定した場合の熱浸透厚さδ(一方の媒質のみへの伝導と考えると式(3))とD_hの大きさにより、$\delta << D_h$では1次元、$\delta >> D_h$で3次元になることが予測できる。$\delta << D_h$の場合、ヒータの熱容量を無

Table 1. Composition of substrate

Case	Solid 1(1.25μm)	Solid 2
I	SiO_2	SiO_2
II	Si	Si
III	SiO_2	Si

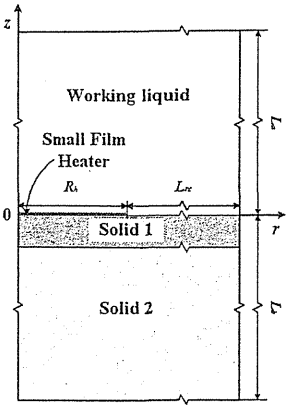

Fig. 1　Schema of simulation area

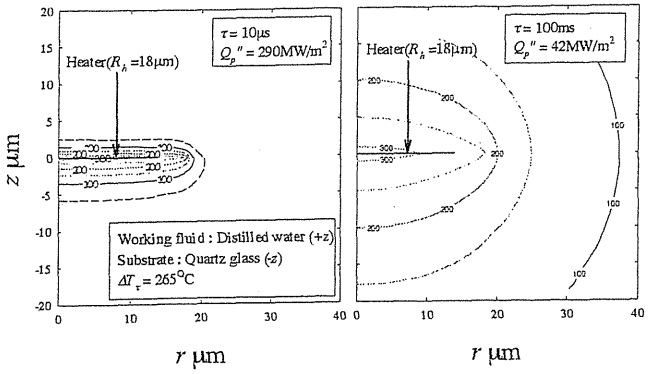

(a) τ = 10μs (b) τ = 100ms

Fig.2 Isotherms around film heater at t=τ

$$\delta = k\frac{\Delta T_\tau}{Q_p''} \quad (3), \quad \Delta T_\tau = \frac{\sqrt{\alpha\tau}}{k\sqrt{\pi}}Q_p'' \quad (4), \quad \frac{\delta}{D_h} = \frac{\sqrt{\alpha\tau}}{D_h\sqrt{\pi}} = \frac{\sqrt{Fo}}{\sqrt{\pi}} \quad (5),$$

$$Q_s'' = \frac{8k}{\pi D_h}\Delta T_a \quad (6), \quad (f_a\tau)\left(\frac{\Delta T_\tau}{\Delta T_a}\right) = \left(\frac{Q_s''}{\Delta T_a}\right)\left(\frac{\Delta T_\tau}{Q_p''}\right) = f(Fo) \quad (7), \quad \Phi = 1 \quad (8),$$

$$\Delta T(\tau) = \frac{2\sqrt{\tau}}{\sqrt{\pi}}Q_p''\times\left(\frac{k_{s,1}}{\sqrt{\alpha_{s,1}}} + \frac{k_l}{\sqrt{\alpha_l}}\right)^{-1} \quad (9), \quad \Phi = \frac{(k_l + k_{s,2})\sqrt{\alpha_l}}{\left(k_l\sqrt{\alpha_{s,1}} + k_{s,1}\sqrt{\alpha_l}\right)}\left(\frac{16}{\pi^{3/2}}\left(\sqrt{Fo}\right)_{s,1}\right) \quad (10)$$

視し基板側への熱伝導だけ考えると、単一パルス加熱時のヒータの温度上昇は式(4)で表され、式(3)を式(4)に代入し、D_hで除して整理すると式(5)が得られる。つまりパルス加熱時のヒータからの放熱が1次元的または3次元的になるかはFo(=$\alpha\tau/D_h^2$)に大きく依存すると考えられる。一方、基板との温度差がΔT_aに保たれた半無限基板上の直径D_hの円板ヒータにおける定常表面熱流束は、2次元熱伝導の形状係数$S=2D_h$より式(6)で表される。式(4)と式(6)をそれぞれ式(2)に代入すると式(7)が得られる。ここで、$f_a\tau(\Delta T_\tau/\Delta T_a)$を無次元許容周波数と呼び、Φで示す。数値計算結果をΦとFoを用いてまとめ、Fig.3に示す。なお、FoはすべてSolid1の熱拡散率αを用いたものである。図から、Φは、パラメータの値によらず、Case I,IIともにそれぞれ一本の線にまとまり、Foの増加とともにその1/2乗に比例して増加し、Fo>1で1に漸近する傾向を示す。Fo<0.1では、$f\propto D_h^{-1}$となるが、これはパルス加熱時の放熱は1次元的であり、式(4)にから分かるようにQ_p''はD_hによらないが、ヒータが小さくなるほど、式(6)よりQ_s''が大きくなるためと考えられる。また、Case IIIにおいてf_aが非常に高くなるのは、SiO_2層の熱拡散率と熱伝導率がSiより二桁以上小さいため、パルス加熱時の温度変化が主にSiO_2層内で生じ、一方連続パルス加熱時の時間平均放熱速度(Q_s'')は、SiO_2層が極めて薄いためSi層に支配されるためと考えられる。

3.2 無次元近似化

前述のΦのFoに対する依存性を考慮して本計算結果に対する無次元近似式を導いた。

i) Foが大きい場合　計算の結果、Foが大きい場合、パルス加熱時の熱伝導もほぼ3次元となり、温度は速やかに常状態に近づくため、パルス加熱中も定常と見なして考え式(6)のQ_s''をQ_p''に、ΔT_aをΔT_τにそれぞれ置き換えた式を(2)のQ_p''に代入し、基板と作動流体の両者への熱移動を考すると式(8)が得られる。Case I,IIにおいてFo>1で計算結がΦ=1に近づくのは同式より理解できる。

ii) Foが小さい場合　パルス加熱時のSolid1と作動流への熱伝導はそれぞれ1次元となり、ヒータの温度上昇は(9)で表される。また繰返しパルス加熱時の時間平均放熱度はほぼSolid2と作動流体によると考えられるので、これを考慮した式(6)と式(9)を式(2)に代入すると式(10)が得られる。ここで、s,1とs,2はそれぞれSolid1とSolid2を意味する以上の式(8)と式(10)はFig.3の破線で示されている。無次元似式による値と数値計算結果はCase I, IIの場合、Fo<$10^{-1}$$Fo$>1の範囲で、Case IIIの場合はFig.3の結果に対しFo<$10^{-1}$$Fo$>$10^{-2}$の範囲で±10%以内でよく一致した。

4. 実験

SiO_2基板上に蒸着された白金薄膜ヒータ(0.1x0.43mm²)をに浸して繰返しパルス加熱実験を行った。試験片、装置及方法は既報[5]と同様である。パルス加熱時間幅2.5μsと10に対して、繰返しパルス加熱を続けても沸騰が起こらない合(非沸騰モード, ΔT_τ≒235K)と、パルス加熱毎に沸騰がきる場合(沸騰モード, ΔT_τ≒265K)のQ_p''をそれぞれ実験よ定め、式(2)から35Kの温度上昇となりうる繰返し加熱周波fを求め、その周波数で繰返し加熱実験を行った。繰返しルス加熱時、パルス加熱直前ヒータに微弱電流を流し、各ルス加熱直前のヒータ温度が時間変化しなくなったときの度(ΔT_a)を測定した。それらから求められた結果をFig.3に沸騰モードを「x」で、沸騰モードを「+」で示す。なお、D_h試験片と加熱面積が等しい230μmとした。無次元近似式にる予測値に対する実験値の差は、非沸騰モードで9%、沸モードで16%以内であった。従って、本モデルにおいて、騰の影響を無視し、またQ_p''とQ_s''によるヒータの温度上昇関するそれぞれの数値計算をもとに式(2)からf_aを求めたこはほぼ妥当と考えられる。

5. 結　言

急速沸騰を用いたマイクロアクチュエータにおける微小ータが許容温度範囲で連続繰返し加熱できる許容周波数を定常熱伝導の数値計算より定め、無次元数でまとめた。まその許容周波数が予測できる無次元近似式を導出した。

【参考文献】(1)加藤ら,特開平11-20148.(2)江刺ら,培風館,(19
2),73.(3)奥山ら,Proc.11th Int. Heat Transf. Conf.(1998),527.(4
奥山ら,TSE,9-6(2001),1.(5)飯田ら,機論(B),63-613(1997), 304

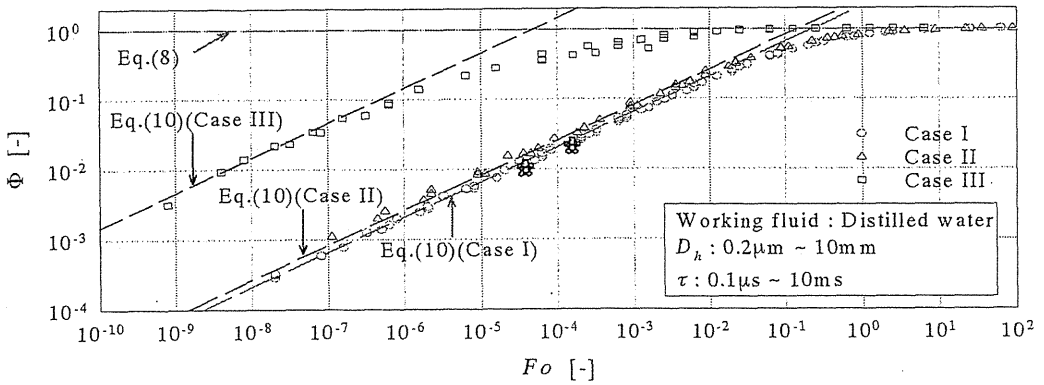

Fig. 3 Non-dimensionalized allowable repetition frequency of pulse heating plotted against Fourier number

Pumping Action by Boiling Propagation Phenomena in a Microchannel

Kunito OKUYAMA, Reo TAKEHARA, Jeong-Hun KIM and Yoshihiro IIDA

Abstract

A prototype micropump which uses boiling propagation phenomena is developed. Boiling is triggered on a film heater which is heated in a pulsewise manner by generating a vapor bubble on a local high heat flux section, and unidirectional boiling propagation is realized over the length of the heater. The heating power conditions under which boiling propagation occurs, configuration of propagation, size of bubbles and propagation velocity are examined. Continuous pumping action in a U-shaped microchannel via boiling propagation repeated at a frequency of up to 20 Hz is demonstrated based on the head difference generated between liquid columns in the vertical sections.

Key Words: Boiling Propagation Phenomena, Micropump

Introduction

Micropumps which use liquid-vapor phase change are receiving increased interest due to advantages such as the absence of mechanically moving parts, large pressure generation and expansion, and high responsivity. Since boiling bubbles generated by the heater placed on the microchannel only repeat the growth and collapse sequence, either a nozzle and/or diffuser structure next to the heater or sequential heating of multiple heaters along the channel are usually needed in order to obtain unidirectional net flow [1-5]. However, these methods make the structure and/or control of the system more complicated.

A new concept for micropumps using phase change is associated with the application of peculiar boiling initiation phenomena which appear when the incipient boiling superheat is much higher than that of steady-state boiling, as is often experiencing for highly wetting liquids. Figure 1 shows high-speed video photographs just subsequent to boiling incipience on a platinum film heater having a width of 1 mm evaporated on a glass plate, immersed in a pool of ethyl alcohol and heated in a stepwise manner at atmospheric pressure and room temperature, together with the time trace of wall superheat. Here, Q , t and ΔT_{sat} denote heating power per unit area of the heater surface, time elapsed after the onset of heating, and wall superheat, respectively. As soon as an initial boiling bubble was generated on the heater at a high wall superheat of approximately 70 K, successive activation of bubble nuclei occurred in the non-boiling region adjacent to the preceding nucleated bubbles, resulting in the rapid coalescing growth of the bubbles along the heated surface such that the bubble area spread over the entire surface. Although the mechanism has not been clarified yet, distortion of temperature distribution in the superheated liquid due to bubble growth may be affecting the induction of boiling in the adjacent region. If boiling propagation is initiated from one end of the heater in a microchannel, of which both the height and width are close to those of the coalesced bubble, as shown in Fig.2, the advancing growth of the bubble toward the other end of the heater and the subsequent receding collapse at the bubble tail may cause a net liquid transport in the direction of the propagation. The authors confirmed the pumping action produced by this phenomena in a microchannel by realizing a unidirectional propagation using a platinum film heater, having a 1 mm × 10 mm area, which was subjected to single-pulse heating [7]. Continuous liquid transport may be feasible by the repetition of boiling propagation using only one heater placed on a straight microchannel having no uneven structure such as nozzle and diffuser.

In the present study, the heating power conditions under which boiling propagation occurs, configuration of propagation, size of bubbles and propagation velocity were investigated using a film heater that is much smaller than that used in Ref.[7]. Pulse heating was repeated at a prescribed frequency under the condition with triggering bubble for the propagation at the end of the heater in a U-shaped microchannel. The resultant pumping action was evaluated based on the head difference generated between the liquid columns in glass capillary tubes.

Experimental apparatus and procedure

Figures 3 and 4 show schematic diagrams of the test section and the experimental apparatus, respectively. The heater is a 0.2-μm-thick platinum film evaporated on a quartz glass substrate having a 0.2 mm × 2 mm heating area. A microchannel having both a height and width of 0.25 mm is constructed on the heater using a thin rubber sheet having a slit and a perforated acrylic resin plate. Glass capillary tubes having an inner diameter of 0.7 mm were vertically connected to the perforations of the resin plate. Thermal ink jet printer ink (without dye), of which the surface tension is approximately 43 mN/m (which is significantly lower than that of water), is poured into the U-shaped channel. A constant pulse current is supplied to the heater at a prescribed frequency using a pulse generator and a power amplifier. Boiling propagation is triggered by the bubble generated at one fine tip (having an area of 0.1 mm × 0.1 mm) of the voltage taps at both ends of the heater via an additional short high pulse when the heater reaches a prescribed superheat for each heating pulse. The timing of the triggering, that is, the duration from the heating onset of the entire heater to the triggering at the tap, was fixed during the repetition of pulse heating. The pumping action was evaluated based on the head difference generated between the liquid columns in the vertical glass tube sections. The pulse power was obtained from the heating current and the voltage drop between the taps, and the heater temperature was obtained from the resistance variation. Boiling bubble behavior was observed using a high-speed video camera having a frame rate of 27000 f/s. The experiment was conducted at room temperature and atmospheric pressure.

Experimental results

Figure 5 shows the wall superheat at boiling incipience under pulse heating without triggering bubble $\Delta T_{sat,B.I.}$ plotted against the pulse power per unit area of the heater surface Q, together with photographs of bubbles immediately after boiling incipience under pool boiling conditions without a channel. Q denotes the time-averaged one over pulse width. Boiling was only initiated at a pulse power higher than 1.3 MW/m^2. The wall superheat is larger than 50 K and increased gradually with the pulse power. A single bubble appeared at an arbitrary location, and the boiling area rapidly spread by propagation over the heater surface at a pulse power lower than 8.3 MW/m^2, whereas at a higher power, several bubbles appeared almost simultaneously, each of which propagated to coalesce with each other.

Figure 6 shows the relationship between bubble height obtained via side observation under pool boiling conditions H_b and wall superheat at boiling incipience. The bubble height increases slightly with the incipient boiling superheat and decreases significantly with an increase in pulse power. The height of the microchannel was set to 0.25 mm so as to be comparable to the bubble height in the case of Q = 4.0 MW/m^2 and was changed to 0.15 mm in the case of Q = 6.5 MW/m^2 by using a thinner rubber sheet.

Figure 7 shows boiling photographs at pulse heating of the entire heater with the generation of triggering bubble at the tap under pool boiling conditions, together with the time traces of the wall

superheat. As soon as the triggering bubble is generated at the tip of the left-hand tap when the wall superheat increases up to the prescribed value (approximately 80 K for case (a) and 98 K for case (b)), boiling was induced on the heater and propagated rapidly to the other end. The propagation was followed by the collapse of the bubble at the tail. Wall superheat decreased significantly due to the heat transfer augmented by boiling. Although the velocity of propagation for case (b) is approximately 2.5 times as large as that in case (a), the configuration of boiling propagation appears to be similar.

Figure 8 shows the average propagation velocity $V_{p,av}$ plotted against the wall superheat at the propagation $\Delta T_{sat,p}$ measured by changing the wall superheat at triggering $\Delta T_{sat,trig}$ under pool boiling conditions. The inception of boiling propagation was delayed slightly following generation of the triggering bubble when $\Delta T_{sat,trig}$ was set to be lower than approximately 60 K. Therefore, $\Delta T_{sat,trig}$ is not always equal to $\Delta T_{sat,p}$. $V_{p,av}$ increases significantly with $\Delta T_{sat,p}$, but appears to be less dependent on Q at a wall superheat higher than 70 K.

Figure 9 shows the time change of the head difference generated between the liquid columns in the glass tube sections Δh during the unidirectional boiling propagation repeated at f = 13 Hz in the microchannel. Δh increases with time to approach the maximum value Δh_{max} at approximately 30 s. The maximum value is maintained during the repetition of pulse heating. After the termination of heating, the head difference decreases gradually to recover to the initial state.

Figure 10 shows the maximum head difference Δh_{max} plotted against the frequency f. Δh_{max} increases markedly with the increases in both f and $\Delta T_{sat,trig}$ up to a maximum of approximately 8.7 mm at f = 20 Hz. In addition, scattering increases with frequency. The increase in Δh_{max} with respect to $\Delta T_{sat,trig}$ may be due to the marked increase in the propagation velocity. However, as the frequency increases further, the head difference decreases abruptly during the repetition of pulse heating, as shown in Fig.11(a) for case of f = 25 Hz. The heater temperature at each pulse heating shifted appreciably higher after one-thousand repetitions of pulse heating, as seen in Fig.11(b), indicating that the substrate temperature around the heater increased significantly for the repeated pulse heating, resulting in the generation of bubbles at random locations along the heater prior to triggering. This may be the reason for the loss of pumping action.

Conclusions

A unidirectional boiling propagation has been realized on the film heater by generating the triggering bubble at the end of the heater for each of the repeated heating pulses. The continuous pumping action by the boiling propagation at a prescribed frequency in the microchannel has been confirmed by the head difference generated between liquid columns in the glass tubes of the experimental apparatus. Pumping at higher frequencies will be enabled by applying a smaller heater and/or choosing the substrate material and composition such that the temperature increase of the substrate would be suppressed during the repetition of pulse heating.

Acknowledgement

This study was supported in part by a Grant-in-Aid for Japan Society for the Promotion of Science (No. 13555053).

Nomenclature

f	repetition frequency of pulse heating, s^{-1}
H_b	height of propagating bubble, m
Δh, Δh_{max}	head difference between liquid columns and maximum head height, m
Q	pulse power per unit area of heater surface, W/m^2
Q_{trig}	triggering pulse power at tip of voltage tap, W/m^2
T_l	liquid temperature, °C
ΔT_{sat}	wall superheat, K
$\Delta T_{sat,B.I.}$	wall superheat at boiling incipience, K
$\Delta T_{sat,p}$	wall superheat during boiling propagation, K
$\Delta T_{sat,trig}$	wall superheat at triggering, K
t	time elapsed after onset of heating, s
$V_{p,av}$	average velocity of boiling propagation, m/s

References

1 P. Gravesen, J. Branebjerg and O.S. Jensen, Microfluidics - a review, J. Micromech. Microeng., vol.3, pp. 168-182, 1993.

2 K. Ozaki, Pumping Mechanism Using Periodic Phase Changes of a Fluid, *Proc.IEEE MEMS*, pp. 31-36, 1995.

3 T.K. Jun and C.J. Kim, Valveless Pumping Using Traversing Vapor Bubbles in Microchannels, *J. Appl. Phys.*, vol.83, no.11, pp. 5658-5664, 1998.

4 H. Yuan and A. Prosperetti, The Pumping Effect of Growing and Collapsing Bubbles in a Tube, *J. Micromech. Microengng.*, vol.9, pp. 402-413, 1999.

5 W.J. Yang, Personal Viewpoint of Heat Transfer - Past, Present and Future -, *Thermal Sci. and Engng.*, vol.9, no.4, pp. 3-8, 2001.

6 K. Okuyama, Y. Iida and T. Kato, Premature Transition to Film Boiling at Stepwise Heat Generation, 2nd Report : Effect of Wall Material and Surface Condition, *Heat Transf. Jap. Res.*, vol.25, pp. 51-63, 1996.

7 K. Okuyama, A. Irikura, R. Takehara, J.H. Kim and Y. Iida, Micropump Using Boiling Propagation Phenomena, *Proc. JSME*, no.01-1, pp. 193-194, 2001.

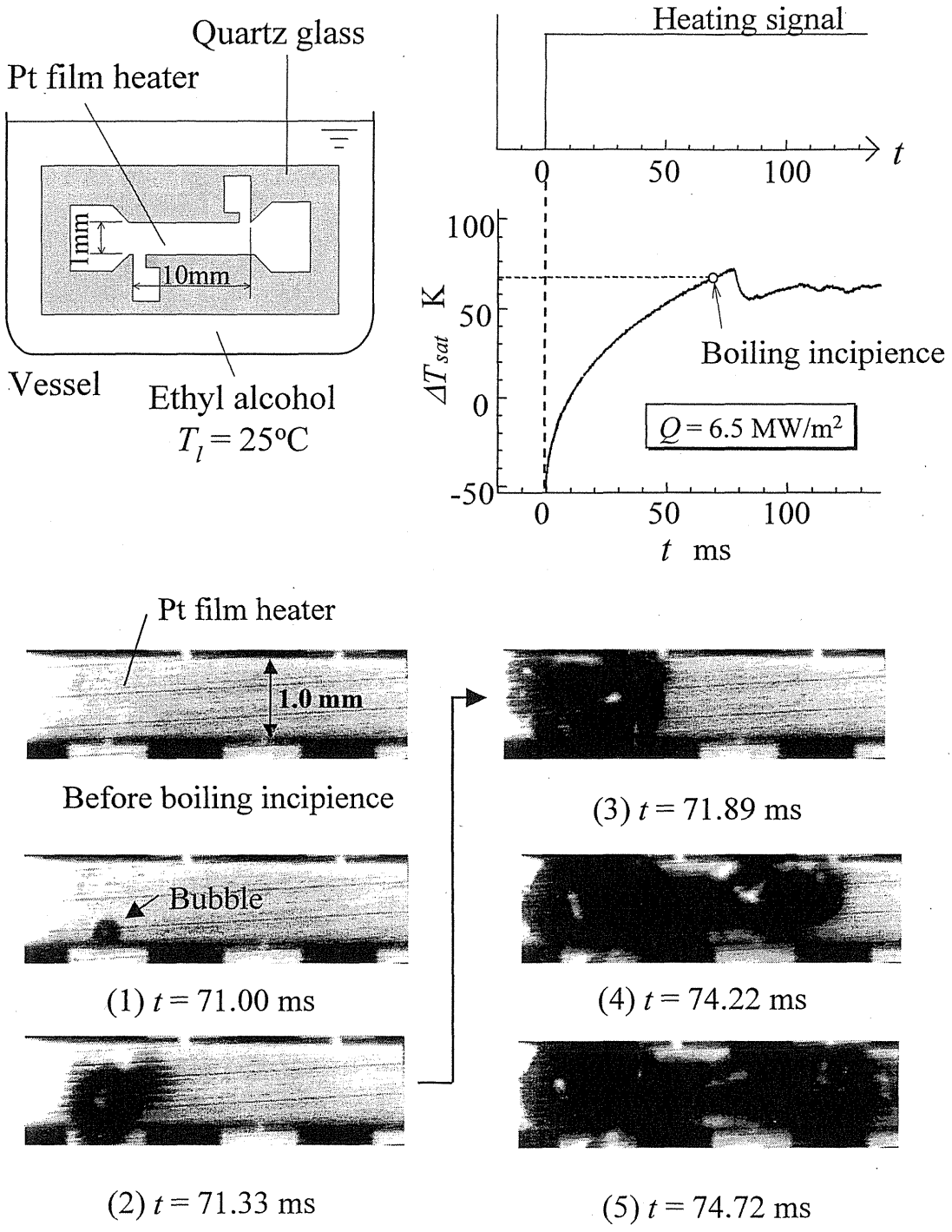

Figure 1 High-speed video photographs just subsequent to boiling incipience on platinum film heater heated stepwise in a pool of ethyl alcohol

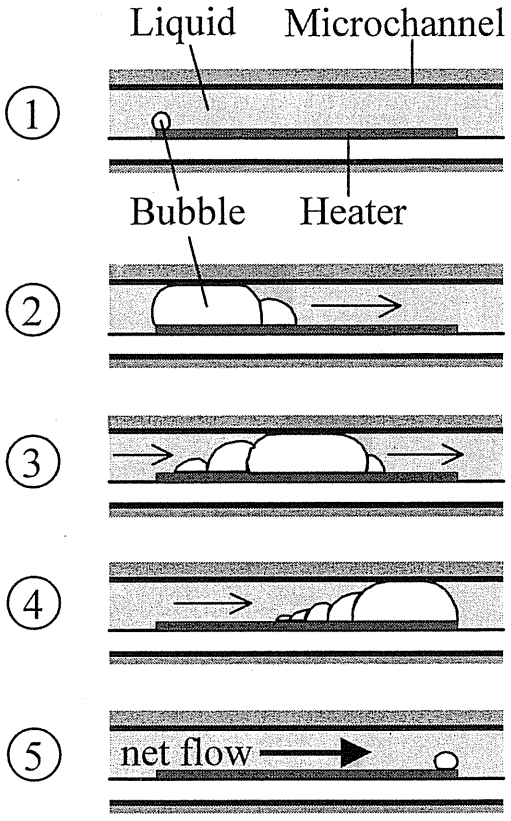

Figure 2 Conceptual boiling propagation initiated from one end of heater and induction of unidirectional liquid flow in microchannel

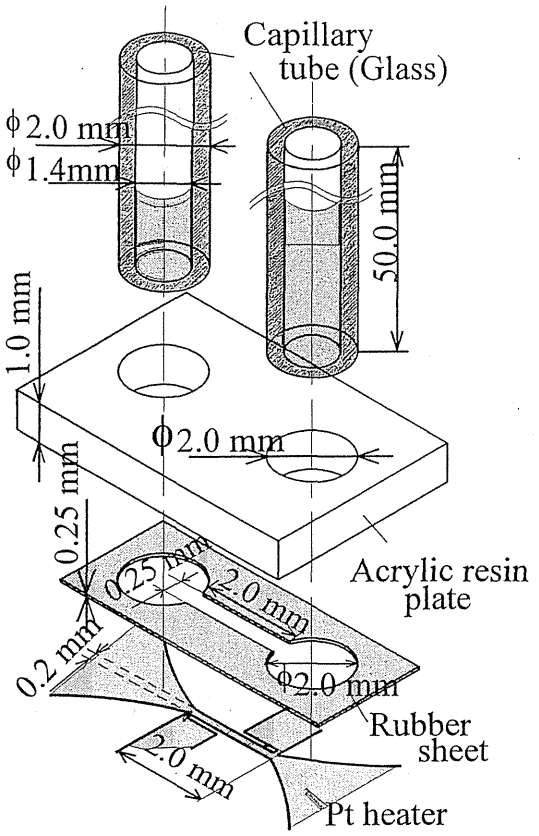

Figure 3 Schematic diagram of the test section

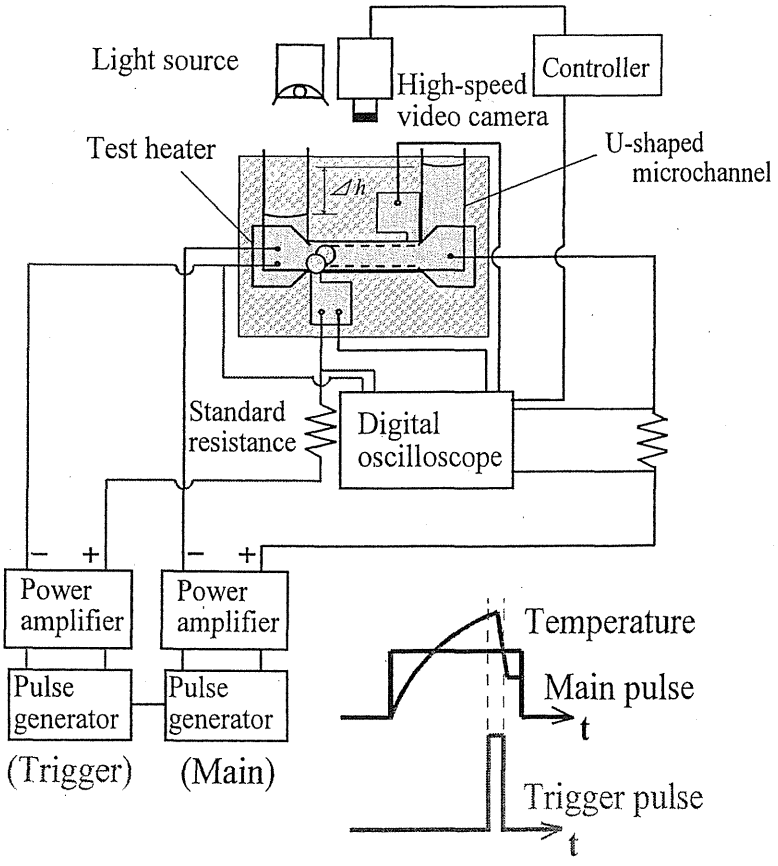

Figure 4 Schematic diagram of experimental apparatus

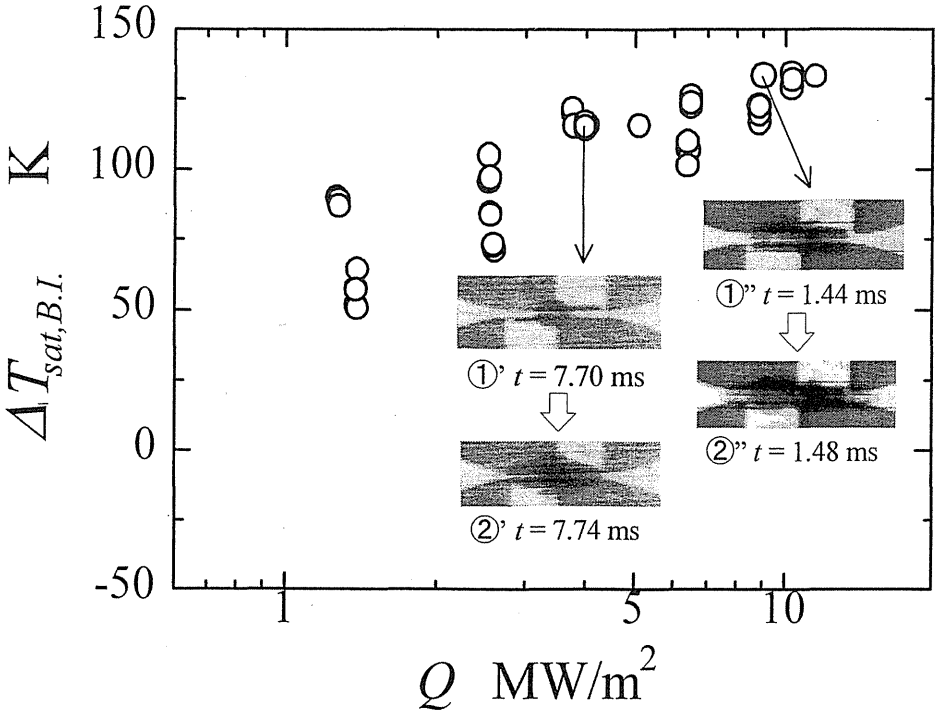

Figure 5 Wall superheat at boiling incipience under pulse heating without triggering bubble plotted against pulse power per unit area of the heater surface

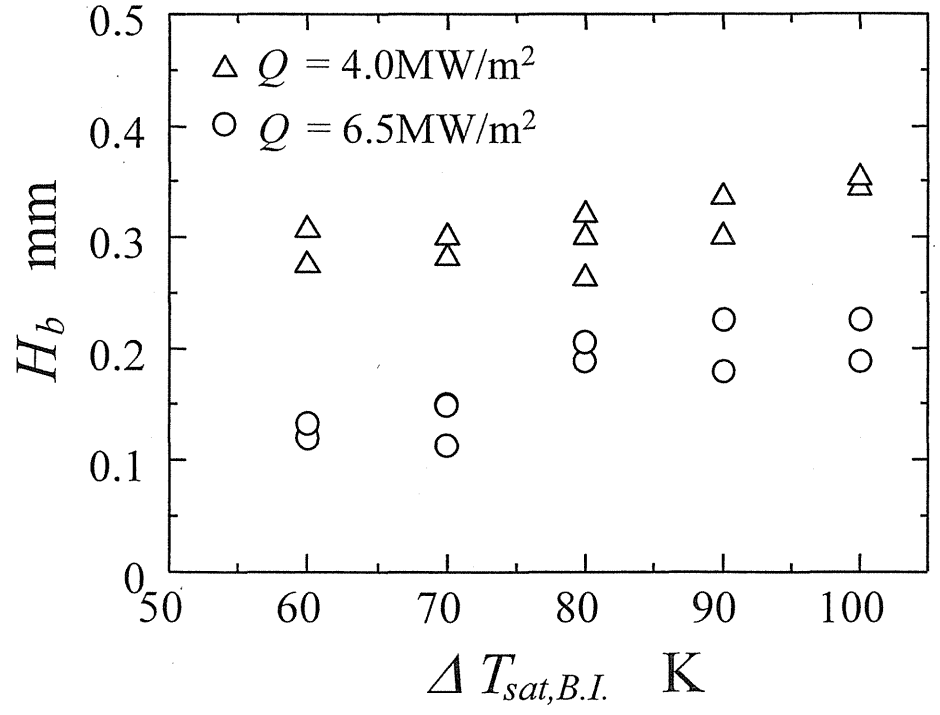

Figure 6 Relationship between bubble height and wall superheat at boiling incipience

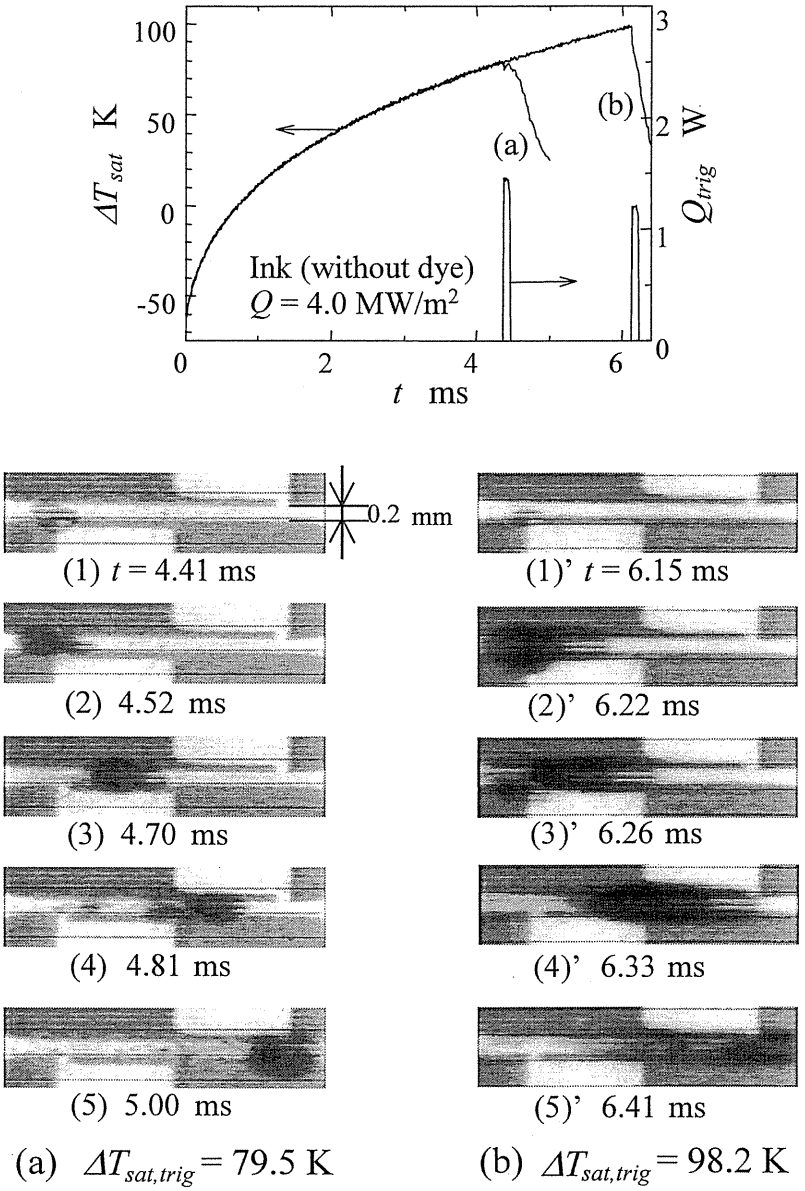

Figure 7 Boiling photographs at pulse heating with triggering bubble in open pool without channel, together with time traces of heater temperature

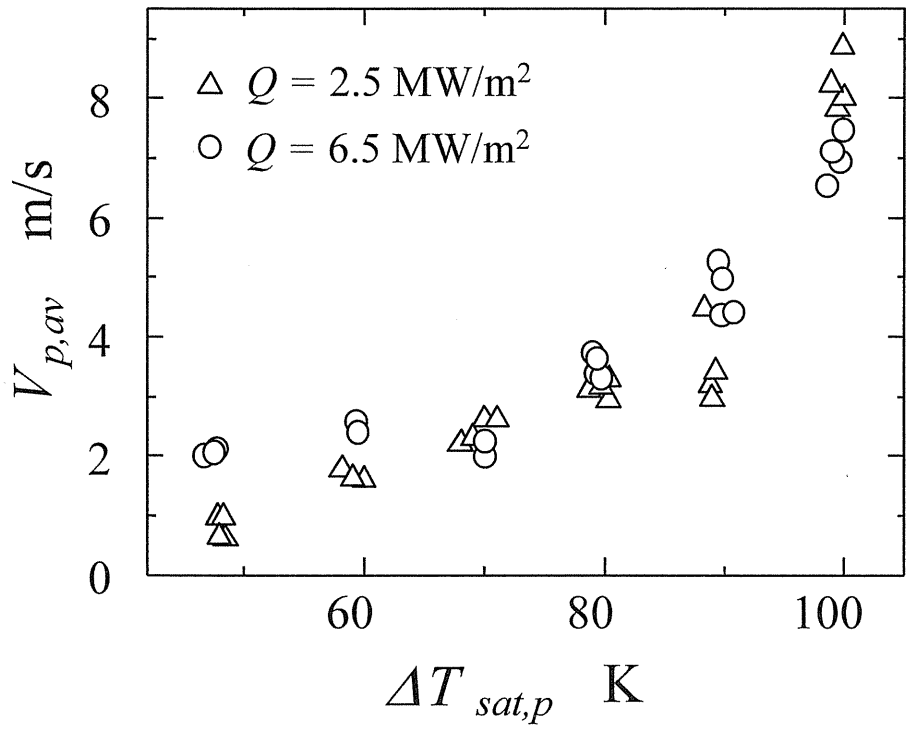

Figure 8 Average propagation velocity $V_{p,av}$ plotted against wall superheat at propagation $\Delta T_{sat,p}$ measured by changing wall superheat at triggering $\Delta T_{sat,trig}$

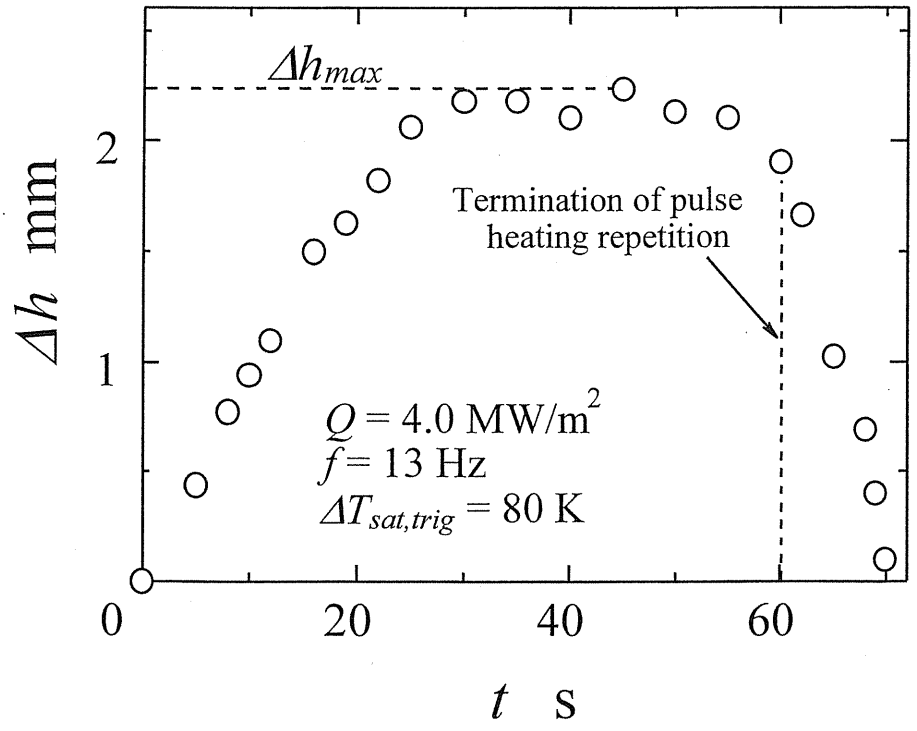

Figure 9 Time trace of head difference generated between liquid columns in glass tubes Δh during unidirectional boiling propagation repeated at f = 13 Hz in microchannel

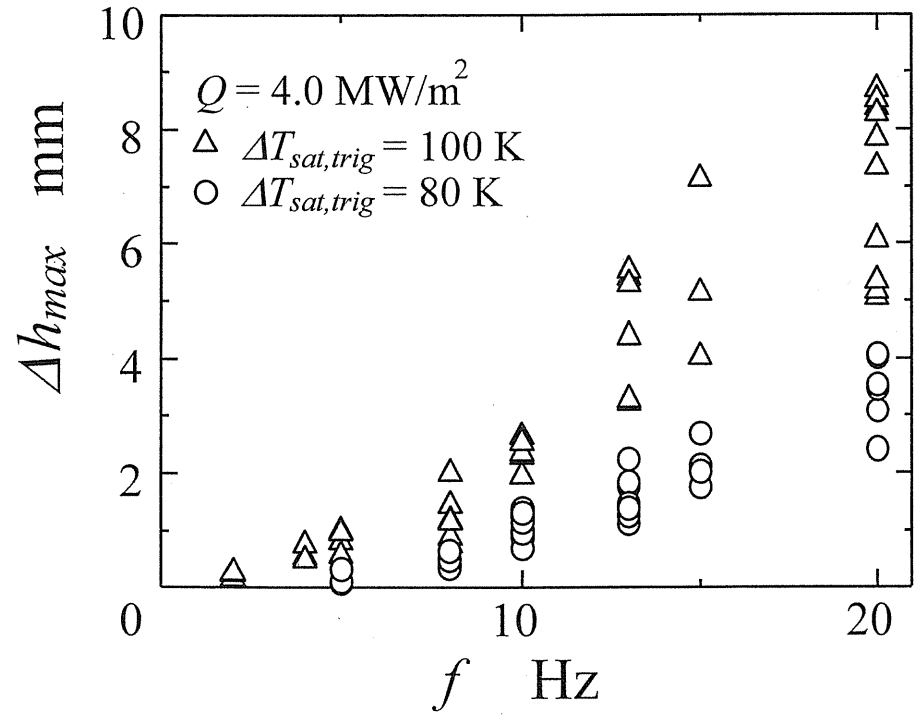

Figure 10 Maximum head difference Δh_{max} plotted against pulse heating repetition frequency f

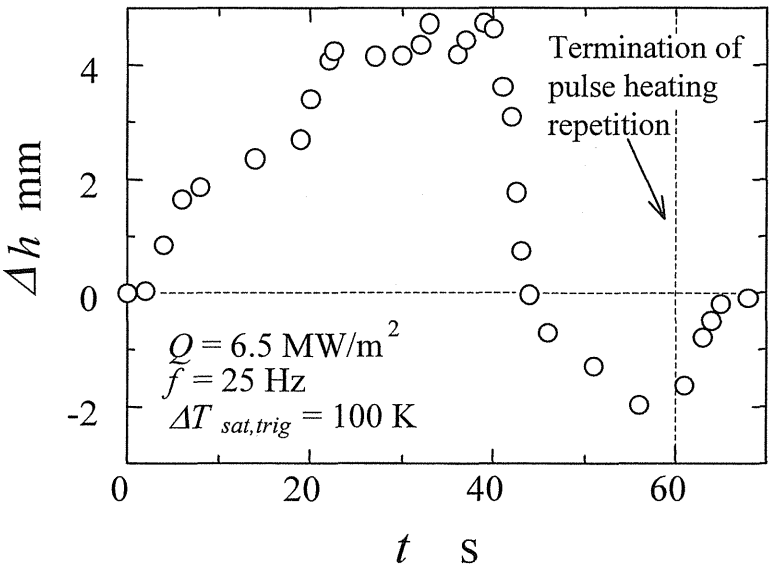

(a)

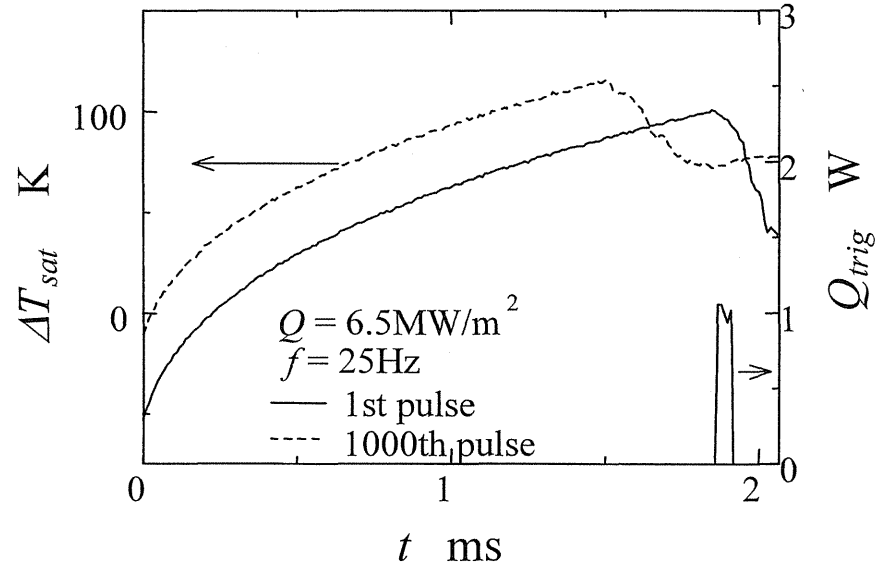

(b)

Figure 11 Time trace of head difference generated between liquid columns Δh during repetition of boiling propagation at $f = 25$ Hz, and wall superheats during the first heating pulse and during the pulse 40 s subsequent to the first pulse

Allowable Repetition Frequency of Pulse Heating in Microactuators Using Rapid Boiling (Effects of heater size and substrate material)

Kunito OKUYAMA , Jeong-Hun KIM and Yoshihiro IIDA

Abstract

High frequency pulse heating of heaters in microactuators utilizing the rapid expansion of boiling bubbles causes a gradual increase in the temperature of the heater and the substrate material in the immediate vicinity of the heater, resulting in a loss of reproducibility of the boiling phenomena. In the present report, the maximum frequency at which the time-averaged increase in the heater temperature can be maintained within allowable limits is obtained from numerical simulations of heat conduction from the heater to adjacent materials using a model in an axisymmetrical system. Instead of direct calculation of the entire repetition process, calculations for two different heating conditions, single pulse heating and steady heating at a time-averaged power during repetition of pulses, are performed. The effects of heater size, pulse width and substrate properties on the allowable frequency are examined and approximate correlations for the allowable frequency are derived in dimensionless form based on an analytical examination. The results show that the allowable frequency increases significantly with a decrease in heater size for prescribed conditions of pulse width and temperature increases during both pulsed heating and steady heating at a time-averaged power. The simulated results are verified by comparison with those from experiments both with and without boiling.

Keywords : Rapid Boiling, Microactuator, Pulse Heating, Allowable Repetition Frequency, Heat conduction, Numerical Simulation

1. Introduction

Microactuators are the key devices in microelectromechanical systems (MEMS) and many designs based on various principles have been proposed and developed over the last two decades. Thermal ink jet (TIJ) printers make use of a type of microactuator that utilizes rapid expansion due to phase change of liquid into vapor[(1)~(4)]. A similar type of microactuators has also been examined for use in the attitude control systems of micro artificial satellites[(5)]. These actuators require a rapid bubble growth and collapse sequence with high reproducibility on a small heater for each high heating pulse. However, pulse heating repeated at high frequencies may cause a significant and gradual increase in the temperature of the heater and substrate adjacent to the heater, which may result in the loss of reproducibility of boiling phenomena and/or damage to the heater due to overheating[(6)~(8)]. In some practical applications, the pulse heating is paused when the substrate temperature exceeds a preset value[(8)].

The allowable frequency, which is the maximum repetition frequency by which the increased (time-averaged) heater temperature can be maintained within allowable limits, may be dependent on the mode of heat diffusion from the heater to adjacent materials as well as the pulse power and pulse width, which are determined from the conditions required for actuation. As the size of the heater is decreased, the three-dimensional effect in the diffusion of heat may become significant in the suppression of the increase in (time-averaged) heater temperature under a prescribed surface heat flux at the heating pulse, resulting in an increase in allowable frequency. Successive actuation at frequencies of the order of 1,000 to 10,000 Hz is enabled in TIJ printers using heaters measuring tens to hundreds of micrometers[(4) (9)].

Heat dissipated in the heater during pulse heating may diffuse into the substrate and liquid by conduction and convection including boiling. However, boiling duration, which can be microseconds to tens of microseconds under pulse conditions for spontaneous nucleation, is usually significantly smaller than the single period of repetition[(9)]. In addition, significant increases in heat transfer due to rapid boiling have only been observed at the instant of bubble collapse, which differs from usual boiling phenomena[(10) (11)]. Moreover, heat conduction, of which the rate is proportional to the characteristic length, becomes relatively significant compared to convection heat transfer, of which the rate is proportional to the square of the characteristic length, according to the scaling law[(12)]. Therefore, the diffusion of heat from the heater to the adjacent materials associated with the temperature increase of the heater during pulse heating can be regarded as dominated by conduction.

In the present study, the maximum frequency with which the steady increase in the time-averaged heater temperature can be maintained within allowable limits during pulse heating is obtained by numerical simulations based on the heat conduction from the heater to adjacent materials. The effects of heater size, pulse width and properties of the substrate on the allowable frequency are examined. Approximate correlations for the allowable frequency are also derived in dimensionless form from analytical examinations. The simulated results are compared with those obtained from experiments both with and without boiling.

2. Nomenclature

c_p specific heat [J/(kg·K)]

D_h	diameter of heater [m]
f	repetition frequency of pulse heating [s^{-1}]
f_a	allowable repetition frequency of pulse heating [s^{-1}]
Fo	Fourier number [–] ($=\alpha\tau/D_h^2$)
k	thermal conductivity [W/(m·K)]
L	length [m]
Q''	heating power per unit heater surface area [W/m^2]
Q_p''	pulse heating power per unit heater surface area [W/m^2]
$Q_p''_{,i}$	heat flux transferred to the medium by pulse heating [W/m^2]
Q_s''	time-averaged heating power per unit heater surface area [W/m^2]
$Q_s''_{,i}$	heat flux transferred to the medium by time-averaged heating [W/m^2]
Q_{so}''	time-averaged heating power per unit heater surface area in case of infinite distances to the outer bounds [W/m^2]
r	coordinate in the radial direction [m]
R_h	radius of heater [m]
S	shape factor for two-dimensional heat conduction [m]
t	time [s]
T_a	allowable limit of heater temperature [°C]
T_h	heater temperature [°C]
T_i	local temperature in media [°C]
T_l	liquid bulk temperature [°C]
T_τ	heater temperature at termination of pulse heating [°C]
ΔT_a	allowable limit of heater temperature increase [K]
ΔT_τ	heater temperature increase at $t = \tau$ during pulse heating [K]
z	coordinate in the perpendicular direction [m]
α	thermal diffusivity [m^2/s]
δ	heat penetration depth [m]
δ_h	thickness of flim heater [m]
Φ	dimensionless allowable frequency [–]($=f_a\tau\,(\Delta T_\tau/\,\Delta T_a)$)
ρ	density [kg/m^3]
τ	pulse width [s]

3. Simulation model and procedure

We consider a small film heater located on the surface of a large substrate being in contact with a sufficient volume of liquid and heated in a pulse-wise manner at a pulse power per unit heater surface area Q_p'', pulse width τ and repetition frequency f. The heater temperature follows a rapid increase and gradual decrease sequence, and the time-averaged heater temperature over a single repetition period gradually increases to reach a constant value after a sufficient time period. However, direct simulation of the entire transient heat conduction process from the heater to the media until the average temperature tends to a steady value requires

calculations over millions of repetitions. Therefore, we consider steady heating at a power averaged over the repetition period Q_s'' expressed as the following equation.

$$Q_s'' = Q_p''\tau f \tag{1}$$

Although the increase in heater temperature at Q_s'' is not equal to that of the time-averaged heater temperature during pulse heating at Q_p'', τ and f, the difference may be insignificant. Therefore, instead of direct calculation of the entire conduction process during pulse repetition, the calculations were performed under two different heating conditions in order to derive the allowable frequency. The first condition states that the transient heating at a single pulse Q_p'' by which the heater temperature increases to the temperature required for boiling initiation T_τ at the time equal to the pulse width, for example spontaneous nucleation temperature of liquid. The other states that steady heating at the time-averaged power Q_s'' by which the time-averaged heater temperature over a single repetition period is regarded to increase to a preset value of allowable temperature T_a. Both power values Q_p'' and Q_s'' were determined via iterative calculation for prescribed temperature increases and the allowable frequency f_a was obtained by substituting these power values and the pulse width into Eq. (1).

Numerical calculations were performed for the model under axisymmetrical conditions, in which the three-dimensional heat diffusion effect can be expressed in a Cartesian co-ordinate system. As shown in Fig.1 a small disk film heater of diameter and thickness D_h (=$2R_h$) and δ_h, respectively, was placed on the surface of a large substrate being in contact with a sufficient amount of liquid. The temperature variation of the heater during heating at Q_p'' or Q_s'' was obtained by solving the transient heat conduction equations for the associated media (Eq. (2)) under the following assumptions:

1. Heat diffusion from the heater to adjacent media only by conduction
2. Constant properties
3. Uniform temperature across the heater film

For the heater

$$\frac{\partial T_h}{\partial t} = \frac{\alpha_h}{r}\frac{\partial}{\partial r}\left(r\frac{\partial T_h}{\partial r}\right) + \frac{Q''}{(\rho c_p)_h \delta_h} \tag{2.a}$$

For the liquid and substrate

$$\frac{\partial T_i}{\partial t} = \frac{\alpha_i}{r}\frac{\partial}{\partial r}\left(r\frac{\partial T_i}{\partial r}\right) + \alpha_i \frac{\partial}{\partial z}\left(\frac{\partial T_i}{\partial z}\right) \tag{2.b}$$

where Q'' is the pulse power Q_p'' for pulse heating and the time-averaged power Q_s'' for steady heating. The subscripts $i = l$ and s denote the liquid and substrate, respectively. These heat conduction equations were discretized according to the finite difference method and then numerical solutions were obtained using a fully implicit scheme under the following initial and boundary conditions[13].

Initial condition:

$$T(r, z, t = 0) = T_l = 25°C \tag{3}$$

Boundary conditions:

$$r = 0 \quad : \frac{\partial T}{\partial r} = 0 \tag{4}$$

$$r = R_h + L_{re} \quad : T(R_h + L_{re}, z, t) = T_l \tag{5}$$

$$z = L_a \quad : T(r, L_a, t) = T_l \tag{6}$$

$$z = L_b \quad : T(r, L_b, t) = T_l \tag{7}$$

where, L_a, L_b and L_{re} are the distances from the heater to the outer boundary of the calculated region and were sufficiently large so as not to affect the increase in heater temperature. For heating at power Q_s'', the power was imposed in a stepwise manner and the calculations continued until the heater temperature reached a steady-state.

The properties of the film heater and the liquid were equal to those of 0.25 μm thick layers of platinum and water, respectively. The properties of the substrate were set to either of two cases, SiO_2 (quartz glass)(Case I) and Si (Case II). D_h was varied from 10 μm to 10 mm. τ was varied from 2.5 μs to 100 ms and 0.5 μs to 10 ms for Case I and Case II, respectively. The temperature increase at time $t = \tau$ for power Q_p'' was set to $\Delta T_\tau (= T_\tau - T_l) = 265$ or 285 K by assuming the value of T_τ around spontaneous nucleation temperature for water. The temperature increase for power Q_s'' was set to $\Delta T_a (= T_a - T_l) = 25$, 40 or 65 K.

4. Results and Considerations

4.1 Results of numerical simulation

Figure 2 shows the calculated allowable frequency plotted against the diameter of the heater for different substrate materials and pulse widths. It can be seen that f_a increases significantly with a decrease in D_h for a prescribed pulse width and tends to saturate at a large pulse width for both substrate cases. The frequency allowed for the silicon substrate (Case II) was much higher than that for the quartz glass substrate (Case I) for the same values of D_h and τ.

In order to understand the systematical effects of these related physical quantities on the allowable frequency, dimensional analysis was performed. Allowable frequency can be correlated to Q_p'', Q_s'' and τ, as seen in Eq. (1), where $Q_p'' = Q_p''(\Delta T_\tau, \alpha, k, D_h, \tau)$ and $Q_s'' = Q_s''(\Delta T_a, k, D_h)$ if the effect of heat capacity of the heater is small. k and α are the thermal conductivity and thermal diffusivity, respectively. For seven independent variables: f_a, τ, D_h, α, k, ΔT_τ and ΔT_a, three independent dimensionless parameters governing the phenomenon were derived as $\alpha\tau/D_h^2$ $(= Fo)$, $(f_a\ \tau)$ and $(\Delta T_\tau / \Delta T_a)$. Here, the product of the latter two is defined as a dimensionless allowable frequency denoted by Φ $(\equiv (f_a\ \tau)(\Delta T_\tau / \Delta T_a))$. Calculated values of f_a over the examined ranges of D_h and τ for both substrates have been plotted in Fig. 3 as the relationship between Φ and Fo, where thermal diffusivity of the substrate material was used to calculate the Fourier number. The results for different values of ΔT_τ and ΔT_a are also shown in the figure. The broken lines represent the prediction by the analytical model described in subsequent section. The dimensionless allowable frequency by the numerical simulation is found to be well correlated with the Fourier number for each substrate case, regardless of the magnitudes of D_h, τ, ΔT_τ and ΔT_a, where Φ increases with an increase in Fo being proportional to the square root of Fo and approaches unity for $Fo > 0.1$.

Figure 4 shows the isotherms around a heater of prescribed size and ΔT_τ at the termination of pulse heating $t = \tau$ for two different pulse widths, which were obtained from the above numerical simulation. The numerals on the isotherms represent the temperature in degrees Celsius. For small values of τ $(Fo = 6.3 \times 10^{-3})$, the temperature variations in the substrate and liquid were restricted in the immediate vicinity of the heater and nearly one-dimensional in the direction normal to the heater surface over a significant part of the surface area.

For large values of τ (Fo = 63), the temperature varied in the media to extend three-dimensionally.

4.2 Analytical considerations

The dependency of the dimensionless allowable frequency on Fourier number at very large or small values as seen in Fig. 3 was examined based on the analytical models. We consider a large substrate with a small film heater disk on its surface, of which both exposed surfaces are thermally insulated (see Fig. 5). The heat penetration depth to the substrate at the termination of pulse heating "δ" can be defined using Eq. (8) under the assumption of one-dimensional heat conduction normal to the heated surface and negligible heat capacity of the heater

$$\delta = k_i \frac{\Delta T_\tau}{Q_p{}''_{,i}} \tag{8}$$

where $Q_p{}''_{,i}$ represents the heating power imposed on the heater, which is equal to the transient heat flux transferred to the medium i (i = l or s). As shown in Fig. 5, heat diffusion to the substrate will become one-dimensional for $\delta << D_h$ and three-dimensional for $\delta >> D_h$ depending on the relative magnitude of δ to D_h. If the heat conduction is one-dimensional and the heat capacity of the heater is negligible, the increase in heater temperature at the termination of pulse heating ΔT_τ can be expressed as the following equation[14].

$$\Delta T_\tau = \frac{2\sqrt{\alpha_i}\sqrt{\tau}}{k_i\sqrt{\pi}} Q_p{}''_{,i} \tag{9}$$

Eliminating ΔT_τ and $Q_p{}''_{,i}$ from Eqs. (8) and (9), we find that the ratio of the heat penetration depth to the heater diameter δ / D_h can be expressed only as a function of the Fourier number Fo (= $\alpha\tau/D_h^2$).

$$\frac{\delta}{D_h} = \frac{2\sqrt{\alpha_i \tau}}{\sqrt{\pi} D_h} = \frac{2\sqrt{Fo}}{\sqrt{\pi}} \tag{10}$$

Under the condition of an extremely large or extremely small Fourier number, analytical expressions to predict the allowable frequency as well as the heater temperature increase can be derived for the system of Fig. 1 in the following way.

1) $Fo << 1$

Heat diffusion from the heater to the substrate and liquid is one-dimensional in the direction normal to the surface. Assuming a negligible heat capacity of the heater and no heat exchange between the substrate and liquid in the region next to the heater ($r > R_h$), the relationship between the pulse heating power Q_p'' and the increase in heater temperature at time $t = \tau$ can be expressed as

$$Q_p{}'' = Q_p{}''_{,s} + Q_p{}''_{,l} = \frac{\sqrt{\pi}}{2\sqrt{\tau}} \left(\frac{k_s}{\sqrt{\alpha_s}} + \frac{k_l}{\sqrt{\alpha_l}} \right) \Delta T_\tau \tag{11}$$

where the subscripts s and l denote the substrate and liquid, respectively. The ratio of heat flux transferred to the liquid to that to the substrate is approximately 0.49 : 0.51 for Case I and 0.09 : 0.91 for Case II from Eq. (9). Under the same assumptions as those for pulse heating, the relationship between a steady heating power Q_s'' and the corresponding heater temperature increase ΔT_a can be expressed by referencing the shape factor for two-dimensional heat conduction systems, $S = 2D_h$[15], as

$$Q_s''=Q_s''_{,s}+Q_s''_{,l}=\frac{8}{\pi D_h}(k_s+k_l)\Delta T_a \tag{12}$$

Substituting Eqs. (11) and (12) into Eq. (1), we obtain the relationship between Φ and Fo.

$$\Phi=\frac{(k_s+k_l)\sqrt{\alpha_l}}{\left(k_s\sqrt{\alpha_l}+k_l\sqrt{\alpha_s}\right)}\left(\frac{16}{\pi^{3/2}}\left(\sqrt{Fo}\right)_s\right) \tag{13}$$

2) $Fo >> 1$

Figure 6 shows the time trace of heater temperature during pulse heating for a prescribed heater size at several different pulse widths. Heating power was adjusted in the calculation so that the heater temperature at time $t = \tau$ was equal. As Fo increases, the heater temperature tends to a steady-state immediately after the onset of heating, which means that the heater temperature is approximately equal to that at the steady-state over the period of the pulse heating width for $Fo >> 1$. Therefore, in the same way as Eq. (12) for Q_s'', the relationship between the heating power Q_p'' and the increase in heater temperature ΔT_τ at $t = \tau$ can be expressed as

$$Q_p''=Q_p''_{,s}+Q_p''_{,l}=\frac{8}{\pi D_h}(k_s+k_l)\Delta T_\tau \tag{14}$$

Substituting Eqs. (12) and (14) into Eq. (1), we obtain

$$\Phi=1 \tag{15}$$

The broken lines in Fig.3 represent the values calculated by Eqs. (13) and (15). These lines are found to be asymptotes for the predicted values by numerical simulation from the figure. The analytical prediction agrees with that of the numerical simulation within ±7% for $Fo < 10^{-2}$ and $Fo > 1$ in the case of a quartz glass substrate (Case I). However, the analytical model predicts values that are slightly smaller than that of the numerical simulations for $Fo < 10^{-4}$ when using an Si substrate (Case II). The deviation in the Si substrate case may be due to the effect of significant heat flow from the substrate to the liquid through the direct contact region next to the heater ($r > R_h$). This is because the thermal conductivity and thermal diffusivity of silicon are two orders of magnitude larger than those of water. Although such an effect was not taken into account in the analytical model, the analytical correlations can predict the results obtained by the numerical simulation within ±10% over the ranges $Fo < 10^{-2}$ and $Fo > 1$ and within ±35% for $10^{-2} < Fo < 1$ for both substrate cases.

The dependence of Φ on Fo in $Fo < 10^{-2}$ ($\Phi \propto Fo^{1/2}$) implies that the allowable repetition frequency varies inversely with heater diameter ($f_a \propto 1/D_h$) over the same range. The heating power (per unit surface area) Q_p'' required for increasing heater temperature up to ΔT_τ at $t = \tau$ is not dependent on heater size as seen in Eq. (11) because heat diffusion from the heater to the media is almost one-dimensional during pulse heating, whereas the steady heating power (per unit surface area) corresponding to the increase in heater temperature is inversely proportional to the heater diameter as seen in Eq. (12). This is because heat diffusion is three-dimensional during steady-state heating. This difference between the dependences of Q_p'' and Q_s'' on heater size may result in an increase in allowable repetition frequency with a decrease in heater size.

When $Fo > 1$, which corresponds to an extremely small heater and/or long pulse width, heat diffusion during pulse heating becomes three-dimensional, which means that Q_p'' is also inversely proportional to D_h, resulting in f_a being independent of D_h. This may be the reason for the saturation tendency of f_a with the decrease in D_h at large pulse widths as seen in Fig. 2.

In actual microactuators, for example TIJ heaters, the value of Fo calculated using the thermal diffusivity of SiO_2, which is the material used for the insulation layer between the heater and silicon substrate, may be within the range 10^{-4} to 10^{-3}.

4.3 Effect of distance to heat sink

As mentioned above, the distances from the heater to the outer bounds of the numerically calculated region L_a, L_b and L_{re}, on which the boundary conditions of the first kind were applied, were assumed to be sufficiently large so as not to affect the heater temperature. However, in practical applications, the distance from the heater to the heat sink must be small. A decrease in the distance may increase the allowable frequency for small values of Fo, causing an increase in the value of Q_s'' for a prescribed temperature increase (see Eq. (1)). Figure 7 shows the ratio of heating power Q_s'' to that in the case of infinite distances to the outer bounds Q_{so}'', as a function of the distance L_a/D_h, where $L_a = L_b = L_{re}$ for Cases I and II. Q_s''/Q_{so}'' increases with a decrease in L_a/D_h by approximately 10% for $L_a/D_h = 1.8$, 30% for $L_a/D_h = 0.9$ and 50% for $L_a/D_h = 0.6$, for both cases. Therefore, the results shown in Fig. 3 will also be valid with an error of less than 10% when the distance from the heater to the heat sink is twice the diameter of the heater.

5. Experimental results

In order to confirm the validity of the numerical simulation, experiments were performed in which a film heater was heated in a pulse-wise manner and the increase in heater temperature was measured. A platinum film heater with a thickness of 0.25 μm and heating area of 100 μm × 400 μm evaporated on a quartz glass substrate with a thickness of 1 mm was placed upwards in a pool of distilled water. It was heated at a prescribed repetition frequency at atmospheric pressure and room temperature (25 °C). The heater temperature was measured via resistance thermometry. The test specimen, experimental apparatus and measurement method were as described previously[16]. Q_p'' was adjusted under single pulse heating to either the power at which ΔT_τ was 235 K such that boiling did not occur during repetition (no-boiling mode) or a slightly larger power at which ΔT_τ was 265 K such that boiling occurred (boiling mode), for pulse widths of 2.5 and 10 μs. The value of Q_s'' was determined such that ΔT_a was 35 K from the steady heating experiment. Pulse heating repetition was performed at the frequency obtained by substituting the power values and pulse width into Eq. (1). The heater temperature was measured immediately before each heating pulse by supplying a small (0.2 A) and short (10 μs) current that did not affect the increase in heater temperature. The dimensionless repetition frequency was estimated by using the steady increase in the measured "before pulse" heater temperature instead of time-averaged value. The diameter of the heater in the Fourier number was assumed to be 230 μm such that the surface area of the heater was equal to that of the test heater.

The experimental results are shown in Fig. 3, where no-boiling mode is indicated by "×" and boiling mode by "+". The difference in the numerical and experimental values of Φ is within 9 % for the no-boiling mode and 16 % for the boiling mode for the same Fourier number. Small deviations in Φ between the boiling and no-boiling modes may imply that boiling occurring as the result of each pulse does not significantly affect the time-averaged increase in heater temperature during pulse heating. From the results shown in the figure, the present model based on the numerical simulation of the heat conduction associated with the temperature increases during both pulse heating and steady heating at a time-averaged power can be concluded to be valid

in the prediction of allowable frequency.

The micro film heaters fabricated by MEMS technology usually have a thin SiO_2 layer between the heating element and silicon substrate. This layer may function so as to increase the allowable repetition frequency of pulse heating as well as to provide electrical insulation. The effect of the layer on the allowable repetition frequency will be examined in detail in future reports.

6. Procedure to calculate allowable frequency

When we calculate the allowable repetition frequency using the numerical results shown in Fig. 3 for a prescribed pulse power Q_p'', it is necessary to be able to obtain the temperature increase ΔT_τ at $t = \tau$ from the values of Q_p'' and τ for an arbitrary size of heater. The temperature increase at pulse heating may be expressed in the functional form of dimensionless quantities according to dimensional analysis

$$\left(\frac{k\Delta T_\tau}{Q_p'' D_h}\right) = g\left(\frac{\alpha\tau}{D_h^2}\right) \tag{16}$$

where $(k\Delta T_\tau)/(Q_p'' D_h)$ and $(\alpha\tau/D_h^2)$ are the dimensionless temperature increase and dimensionless heating time, respectively, and g denotes a function. After a sufficiently large heating period, at which the situation reduces to that of steady-state heating, the temperature increase may be expressed in terms of the temperature increase ΔT_a and power Q_s'' as

$$\left(\frac{k\Delta T_a}{Q_s'' D_h}\right) = C \tag{17}$$

where C is a constant having a value close to $\pi/8$ (refer Eq. (12)). Substituting Eqs. (16) and (17) into Eq. (1), we get

$$\Phi = (f_a\tau)\left(\frac{\Delta T_\tau}{\Delta T_a}\right) = \frac{1}{C} g\left(\frac{\alpha\tau}{D_h^2}\right) = \frac{1}{C}\left(\frac{k\Delta T_\tau}{Q_p'' D_h}\right) \tag{18}$$

Equation (18) implies that the dimensionless allowable repetition frequency changing with the Fourier number (shown in Fig. 3) is proportional to the temperature increase of the heater during a single heating pulse.

Figure 8 shows several time variations of temperature increase during pulse heating by the numerical simulations (solid lines), which are depicted in terms of dimensionless quantities appearing in Eq. (18). The thermal conductivity in the dimensionless temperature increase was expressed in the summed form $(k_s + k_l)$ considering heat conduction to both materials. The allowable frequencies obtained by the simulation in Fig. 3 are also plotted in the figure. Temperature increases at different heater sizes and heating powers are well correlated only by the Fourier number for both the substrate cases and agree with the allowable frequencies over the range $Fo > 10^{-3}$ to within ±6%. The disagreement in the range $Fo < 10^{-3}$ may be due to the heat capacity of the heater. The effect of heat capacity on temperature increase during pulse heating is significant only in the early stages and reduces with time. In the simulation for the allowable frequency, the pulse width was set so as to be sufficiently long.

To summarize, in the calculation of the allowable frequency, we first choose the substrate and liquid

materials, and assume values of heater size D_h, pulse heating power Q_p'', pulse period τ and temperature increase ΔT_a. Next, we obtain the temperature increase ΔT_τ and dimensionless allowable frequency Φ using Fig. 8 and Fig. 3, respectively, for the corresponding Fourier number. The value of allowable frequency f_a is calculated from the definition of Φ.

7. Conclusions

The maximum frequency at which the increase in time-averaged heater temperature can be maintained below an allowable limit during pulse heating in microactuators using rapid boiling has been predicted based on a numerical simulation of heat conduction from a heater to adjacent materials. The calculations were performed for single pulse and steady heating at a time-averaged power instead of direct calculation of the entire repetition process. The results show that the allowable frequency increases significantly with a decrease in heater size for prescribed conditions of pulse width and temperature increases during both pulsed heating and steady heating at a time-averaged power. The frequency tends to saturate with a decrease in heater size for long pulse widths.

The effects of heater size, pulse width and properties of substrate on the frequency have been correlated over wide ranges in terms of the dimensionless quantities governing the phenomenon. In addition, approximate correlations for the allowable frequency in dimensionless form, which well predict the frequency by numerical simulation in the ranges $Fo < 10^{-2}$ and $Fo > 1$, have been derived.

The simulated repetition frequency agrees with the results obtained from experiments both with and without boiling. The present model, in which the cooling effect due to boiling and natural convection was disregarded, will be valid for the prediction of allowable frequency.

References

(1) Allen, R.R., Meyer, J.D. and Knight, W.R., Thermodynamics and Hydrodynamics of Thermal Ink Jets, *Hewlett-Packard J.*, Vol. 36, No. 5 (1985), pp. 21-27.

(2) Asai, A., Hara, T. and Endo, I., One-Dimensional Model of Bubble Growth and Liquid Flow in Bubble Jet Printers, *Jpn. J. Appl. Phys.*, Vol. 26, No. 10 (1987), pp. 1794-1801.

(3) Asai, A., Bubble Dynamics in Boiling under High Heat Flux Pulse Heating, *J. Heat Transf.*, Vol. 113 (1991), pp. 973-979.

(4) Chen, P.H., Chen, W.C., Ding, P.P. and Chang S.-H., Bubble Growth an Ink Ejection Process of a Thermal Ink Jet Printhead, *Int. J. Mech. Sci.*, Vol. 39, No. 6 (1998), pp. 683-695.

(5) Ye, X.Y., Tang, H.Q. and Zhou, Z.Y., Study of a Vaporizing Water Micro-thruster, *Sensors and Actuators A*, Vol. 89 (2001), pp. 159-165.

(6) Okuyama, K., Takehara, R., Kim, J.-H. and Iida, Y., Micropump Using Boiling Propagation Phenomena, *Thermal Sci. & Eng.*, Vol. 10, No. 4 (2002), pp. 19-20.

(7) Masaki, T., Japan Patent, H9-239989 (in Japanese).

(8) Kato, M., Japan Patent, H11-20148 (in Japanese).

(9) Okuyama, K., Morita, N., Maeda, A. and Iida, Y., Removal of Residue on Small Heaters Used in TIJ Printers by Rapid Boiling, *Thermal Sci. & Eng.*, Vol. 9, No. 6 (2001), pp. 1-7.

(10) Okuyama, K. and Iida, Y., Boiling Bubble Behavior and Heat Transfer Succeeding Spontaneous Nucleation on a Film Heater, Heat Transfer 1998, *Proc. 11th Int. Heat Transf. Conf.*, No. 2 (1998), pp. 527-532.

(11) Iida, Y., Okuyama, K. and Nishizawa, T., Heat transfer during Boiling Initiated by Fluctuation Nucleation on a Platinum Film Rapidly Heated to the Limit of Liquid Superheat (1st Report, Experiment under Atmospheric Pressure Condition), *Trans. Jpn. Soc. Mech. Eng.*, (in Japanese), Vol. 63, No. 613, B (1997), pp. 3048-3054.

(12) Esashi, M., Fujita, H., Igarashi, I. and Sugiyama, S., Micromachining and Micro Electronics, (in Japanese), Baifukan, Tokyo, (1992), pp. 73-89.

(13) Patankar, S.V., Numerical Heat Transfer and Fluid Flow, Hemisphere Publishing Corporation, New York, (1980), pp. 22-42.

(14) Carslaw, H.S. and Jaeger, J.C., Conduction of Heat in Solids, Oxford University Press, London, (1959), pp. 75-77.

(15) Incropera, F.P. and DeWitt, D.P., Fundamentals of Heat and Mass Transfer, John Wiley & Sons, Inc., New York, (1996), pp. 196-171.

(16) Iida, Y., Okuyama, K. and Sakurai, K., Boiling Nucleation on a Very Small Film Heater Subjected to Extremely Rapid Heating, *Int. J. Heat Mass Transf.*, Vol. 37, No. 17 (1994), pp. 2771-2780.

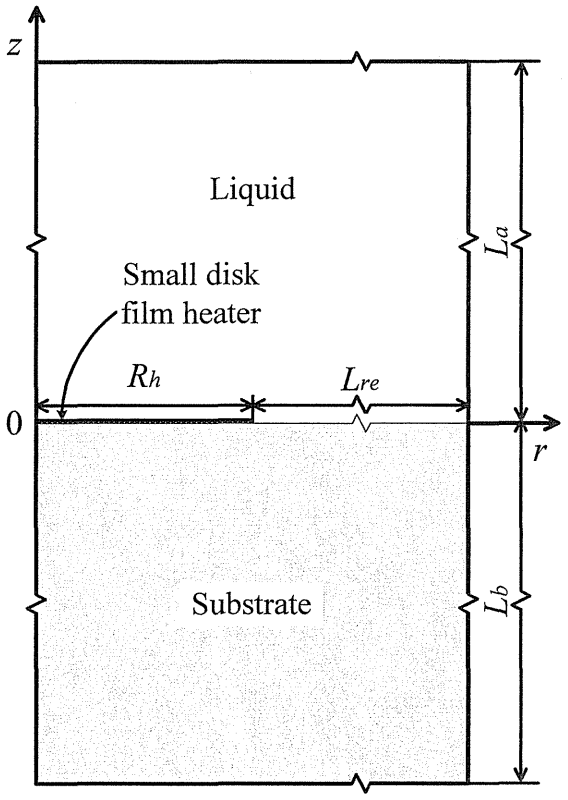

Fig. 1 Simulation area

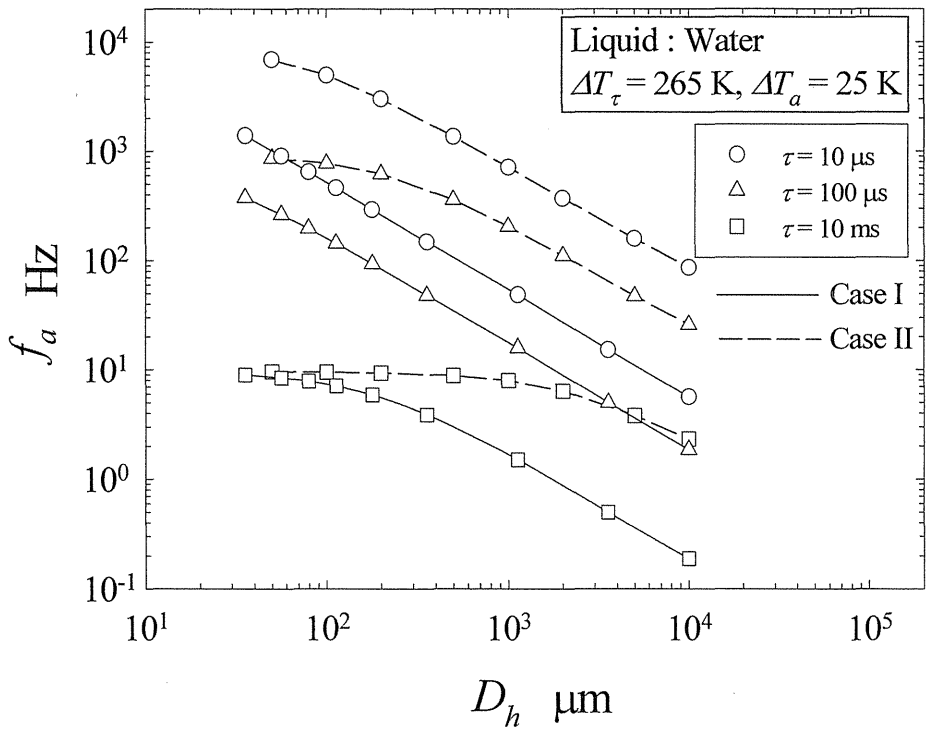

Fig. 2 Allowable repetition frequency as a function of heater diameter

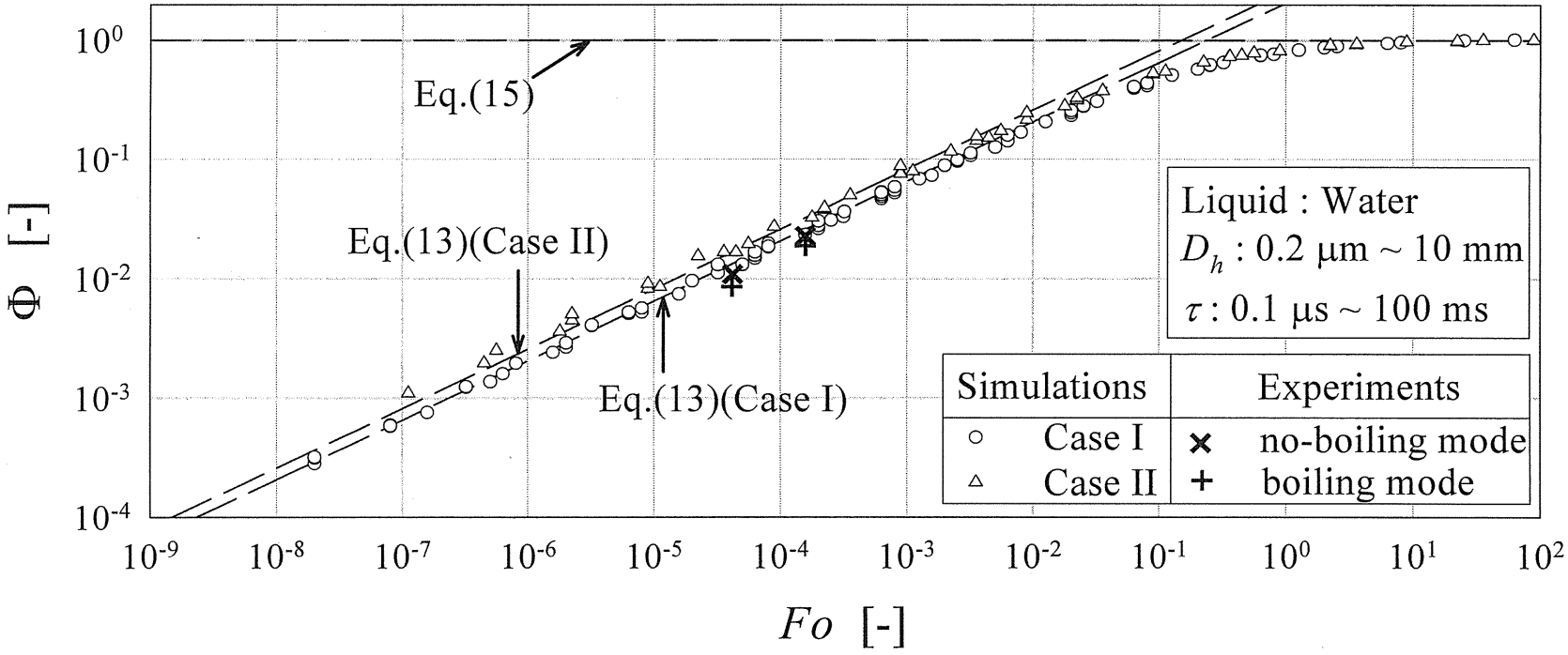

Fig. 3 Dimensionless allowable repetition frequency of pulse heating against Fourier number

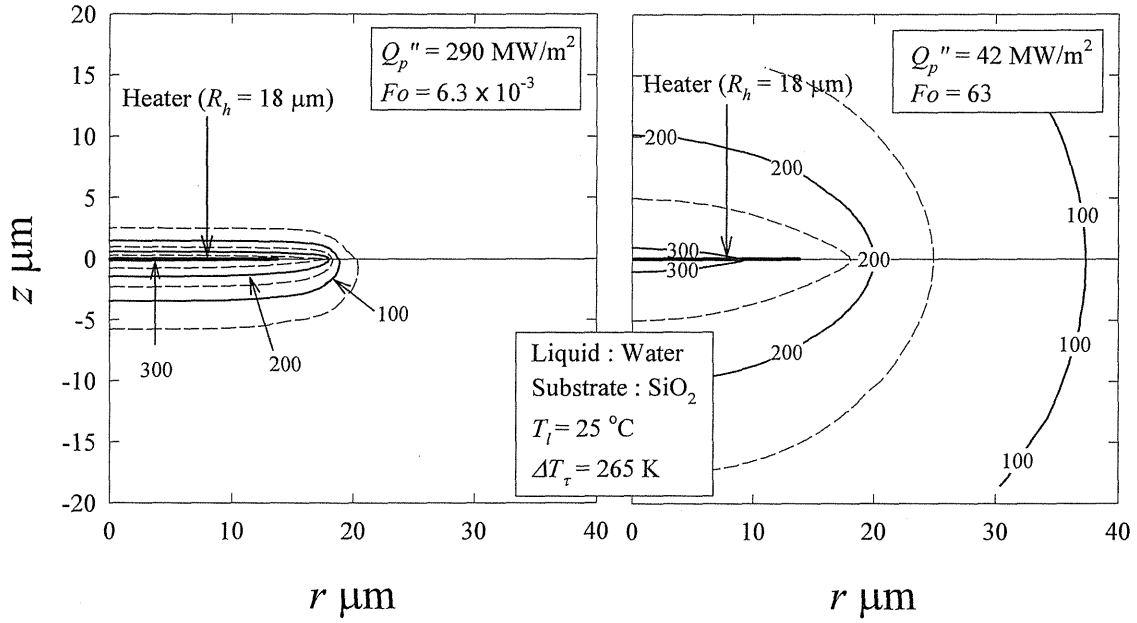

(a) $\tau = 10$ μs (b) $\tau = 100$ ms

Fig. 4 Isotherms around film heater at the termination of pulse heating $t = \tau$

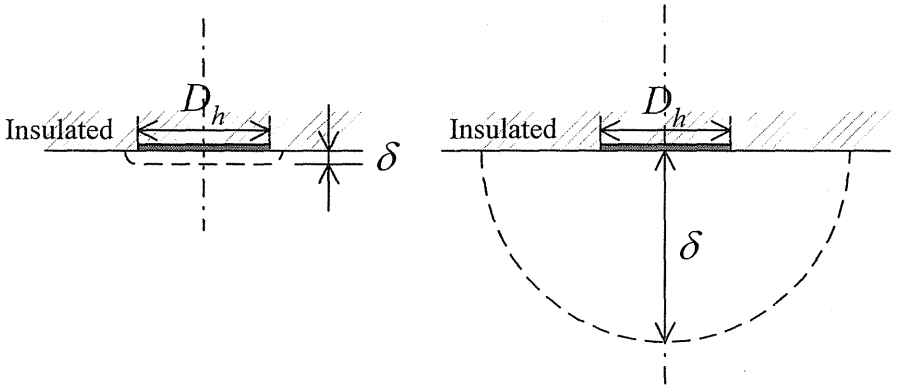

(a) $\delta << D_h$ (b) $\delta >> D_h$

Fig. 5 Heat penetration depth to the substrate at different terminations of pulse heating $t = \tau$

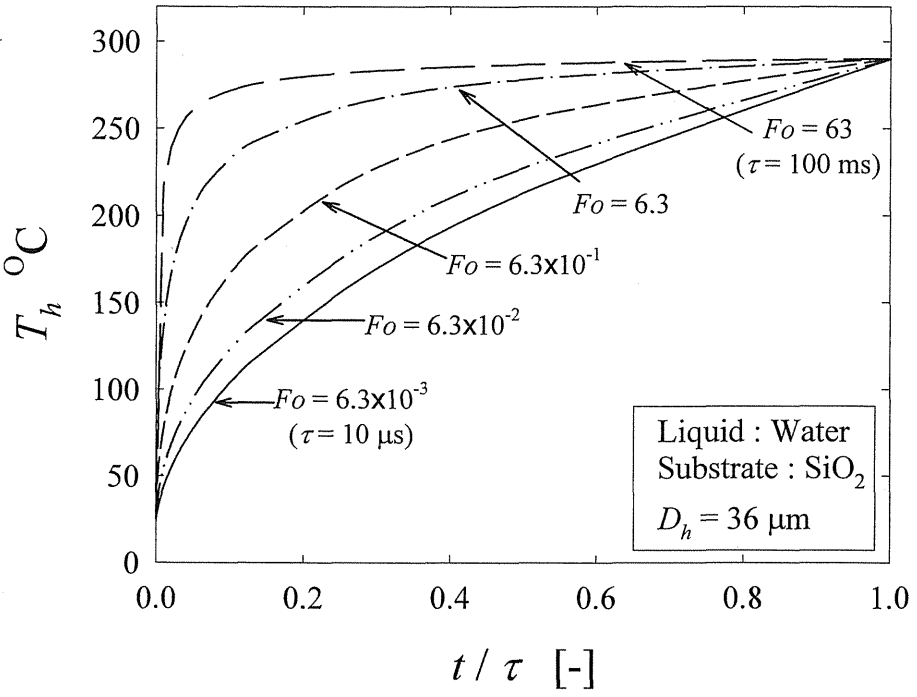

Fig. 6 Time variation of heater temperature at several different pulse widths

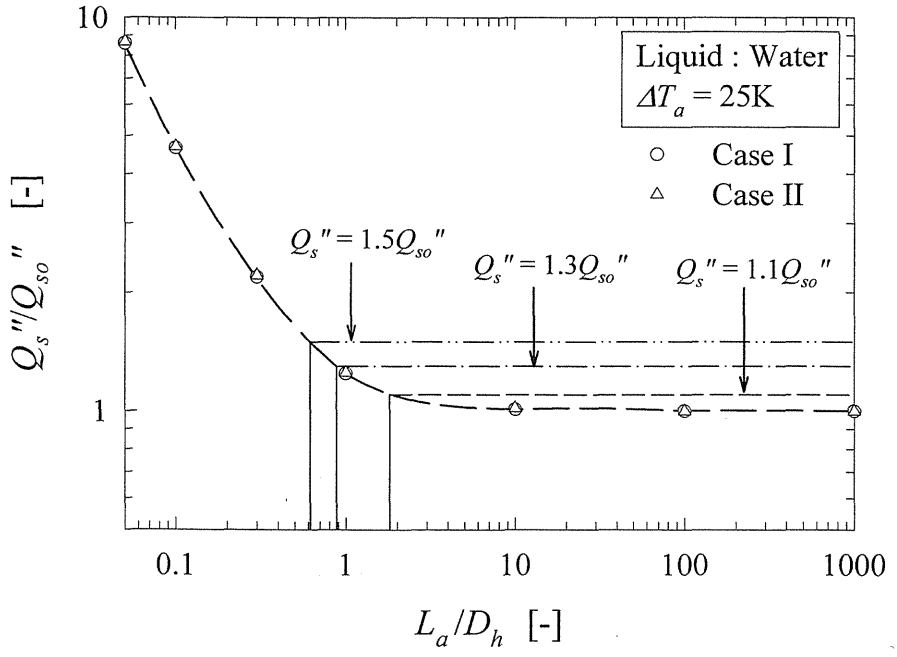

Fig. 7 Heating power ratio as a function of dimensionless distance from heater to heat sink

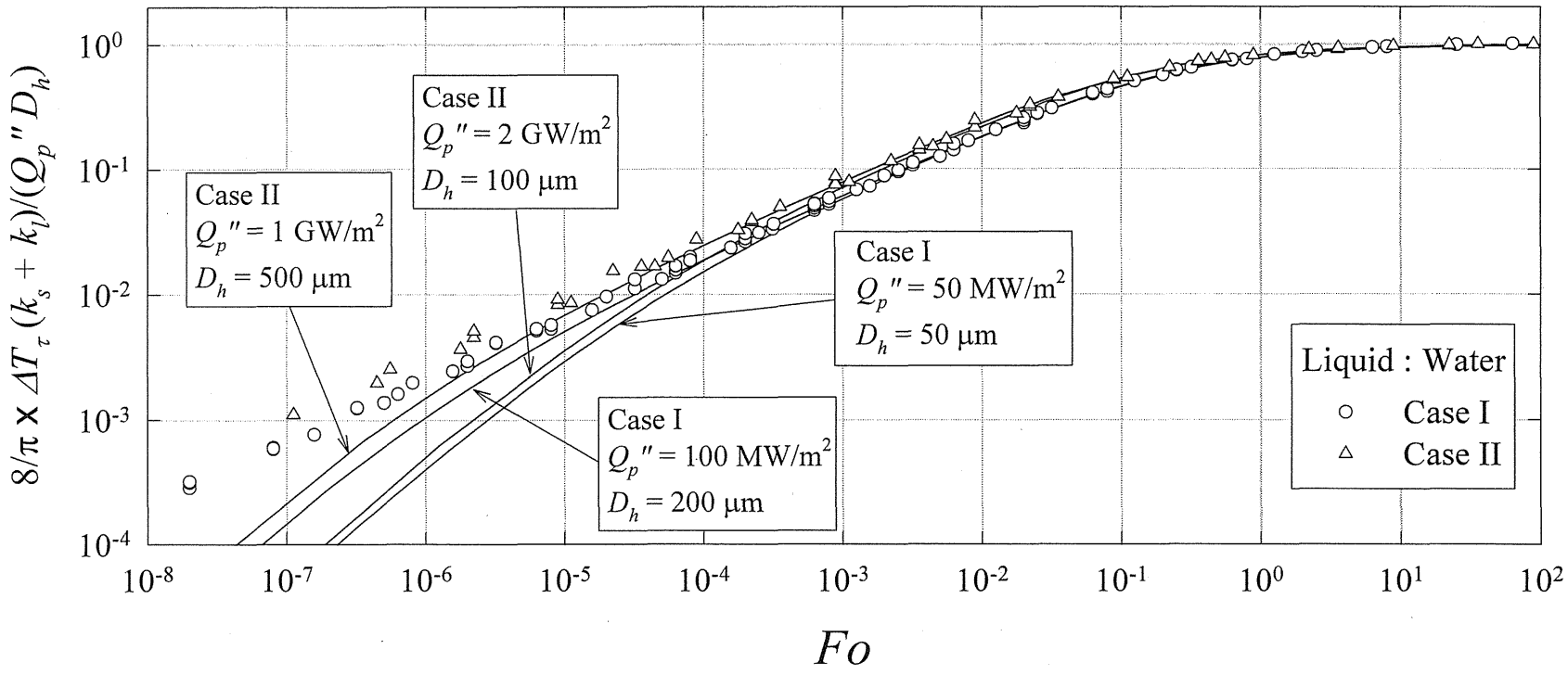

Fig. 8 Dimensionless temperature increase against Fourier number